# Style and Rate of Quaternary Deformation of the Hosgri Fault Zone, Offshore South-Central California

Edited by Margaret A. Keller

Chapter BB of

**Evolution of Sedimentary Basins/Offshore Oil and Gas Investigations—Santa Maria Province**

By Kathryn L. Hanson, William R. Lettis, Marcia K. McLaren, William U. Savage, and N. Timothy Hall

Bulletin 1995–BB

U.S. Department of the Interior
U.S. Geological Survey

**U.S. Department of the Interior**
Gale A. Norton, Secretary

**U.S. Geological Survey**
Charles G. Groat, Director

Version 1.0, 2004

This publication is available only online at:
**http://pubs.usgs.gov/bul/b1995-bb/**

Text edited by James W. Hendley II
Layout by Stephen L. Scott
Manuscript approved for publication, July 27, 2004

# Contents



## Figures

## Figures



## Tables

# Style and Rate of Quaternary Deformation of the Hosgri Fault Zone, Offshore South-Central California

By Kathryn L. Hanson,[1] William R. Lettis,[2] Marcia K. McLaren,[3] William U. Savage,[4] and N. Timothy Hall[1]

## Abstract

The Hosgri Fault Zone is the southernmost component of a complex system of right-slip faults in south-central coastal California that includes the San Gregorio, Sur, and San Simeon Faults. We have characterized the contemporary style of faulting along the zone on the basis of an integrated analysis of a broad spectrum of data, including shallow high-resolution and deep penetration seismic reflection data; geologic and geomorphic data along the Hosgri and San Simeon Fault Zones and the intervening San Simeon/Hosgri pull-apart basin; the distribution and nature of near-coast seismicity; regional tectonic kinematics; and comparison of the Hosgri Fault Zone with worldwide strike-slip, oblique-slip, and reverse-slip fault zones. These data show that the modern Hosgri Fault Zone is a convergent right-slip (transpressional) fault having a late Quaternary slip rate of 1 to 3 mm/yr. Evidence supporting predominantly strike-slip deformation includes (1) a long, narrow, linear zone of faulting and associated deformation; (2) the presence of asymmetric flower structures; (3) kinematically consistent localized extensional and compressional deformation at releasing and restraining bends or steps, respectively, in the fault zone; (4) changes in the sense and magnitude of vertical separation both along trend of the fault zone and vertically within the fault zone; (5) strike-slip focal mechanisms along the fault trace; (6) a distribution of seismicity that delineates a high-angle fault extending through the seismogenic crust; (7) high ratios of lateral to vertical slip along the fault zone; and (8) the separation by the fault of two tectonic domains (offshore Santa Maria Basin, onshore Los Osos domain) that are undergoing contrasting styles of deformation and orientations of crustal shortening. The convergent component of slip is evidenced by the deformation of the early-late Pliocene unconformity. In characterizing the style of faulting along the Hosgri Fault Zone, we assessed alternative tectonic models by evaluating (1) the cumulative effects of multiple deformational episodes that can produce complex, difficult-to-interpret fault geometries, patterns, and senses of displacement; (2) the difficult imaging of high-angle fault planes and horizontal fault separations on seismic reflection data; and (3) the effects of strain partitioning that yield coeval strike-slip faults and associated fold and thrust belts.

## Introduction

Characterizing the sense of slip, slip rate, and down-dip geometry of the Hosgri Fault Zone has been the subject of much research and debate since the fault was first identified as a significant structure within the offshore Santa Maria Basin by Wolf and Wagner (1970) and Hoskins and Griffiths (1971). The Hosgri Fault Zone, sensu stricto, excluding the San Simeon Fault Zone, which we consider to be a geologically distinct part of the system, is offshore along its entire 110-km length (fig. 1). It extends from Estero Bay on the north, where the fault forms a 5-km-wide stepover with the San Simeon Fault Zone (Di Silvestro and others, 1990; Lettis and others, 1990; Willingham and others, this volume) to near Point Pedernales, where it dies out along the offshore projection of the northwestern margin of the western Transverse Ranges (Cummings and Johnson, 1994; Willingham and others, this volume). The fault zone, which generally consists of two north-northwest-trending linear strands (fig. 2), forms a major structural boundary between the 2- to 3-km-thick, mildly deformed Neogene section of the offshore Santa Maria Basin to the west and the west-northwest-trending, highly folded and faulted rocks of the Los Osos domain of the southern Coast Ranges to the east (Lettis and others, 1989, this volume). Geomorphic expression of the fault by inflections, steps, and scarps in the sea-floor, disruptions of the post-late Wisconsin unconformity (~18 ka), and mismatched post-late Wisconsin sediment thicknesses across the fault demonstrate late Quaternary tectonic activity along the zone (Wagner, 1974; Leslie, 1981; Niemi and others, 1987; Pacific Gas and Electric Company (PG&E), 1988) and show that this structure is

[1] Geomatrix Consultants, Inc., Oakland, CA 94612.
[2] William Lettis & Associates, Inc., Walnut Creek, CA 94596.
[3] Pacific Gas and Electric Company, San Francisco, CA 94177.
[4] U.S. Geological Survey, Menlo Park, CA 94025 (formerly with Pacific Gas and Electric Company).

currently accommodating strain within the current transpressional regime of the plate boundary region. Characterization of the contemporary style and rate of deformation along this structure, therefore, is critical to understanding the regional neotectonic setting of south-central coastal California.

In this paper we examine the late Quaternary behavior of the Hosgri Fault Zone. Our understanding of its sense of slip is based on a multidisciplinary examination of the zone and the associated San Simeon Fault Zone to the north. Our analysis includes the integration of a wide variety of data, including shallow high-resolution and deep-penetration common depth point (CDP) seismic reflection data along the entire length of the fault zone; geologic and geomorphic data along the Hosgri Fault Zone, the San Simeon Fault Zone, and the intervening San Simeon/Hosgri pull-apart basin; the distribution and nature of seismicity; consideration of regional tectonic kinematics; and comparison of the characteristics of the Hosgri Fault Zone with worldwide examples of strike-slip, oblique-slip, and reverse fault zones. This work was contracted by the Pacific Gas and Electric Company (PG&E), who along with professional development programs of Geomatrix Consultants, Inc., and William Lettis and Associates, Inc., supported its completion for this publication. A detailed description of the geophysical data sets, which are an integral part of this analysis, is presented by Willingham and others (this volume). An overview of the Hosgri Fault Zone in the regional tectonic kinematic setting is provided by Lettis and others (this volume).

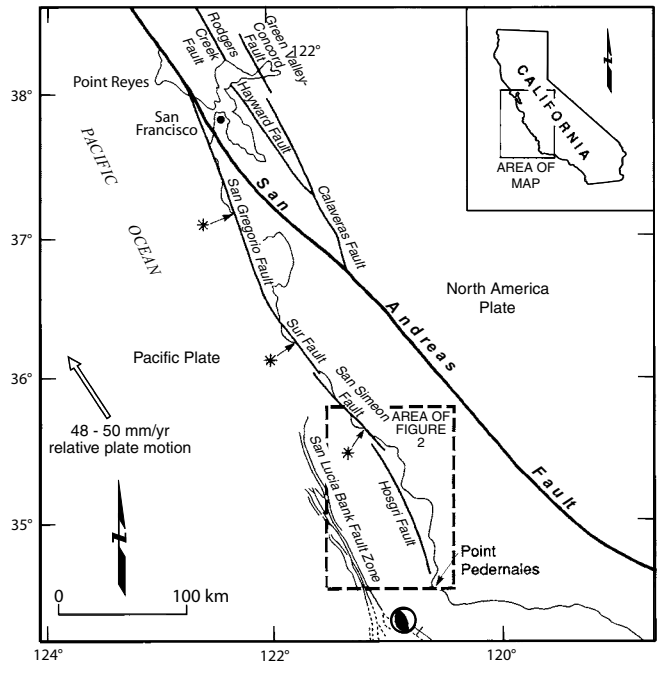


Figure 1. The Hosgri Fault Zone, which lies within the transpressional plate margin of south- central coastal California, is the southernmost component of the San Gregorio/ Hosgri fault system. This complex system of faulting, which is subparallel to the central California coast, splays off the San Andreas Fault between Point Reyes and San Francisco on the north (Jennings, 1975) and appears to die out approximately 410 km to the southeast near Point Pedernales. Detailed mapping and paleoseismic investigations at onshore localities (shown by asterisks) document the Quaternary right-slip behavior of the northern three-quarters of the fault system and show that it is accommodating a small amount of the relative plate motion (DeMets and others, 1990) between the Pacific and North American Plates (indicated by large arrow). The location and focal mechanism of the November 4, 1927, $M_S$ 7.0 Lompoc earthquake is from Helmberger and others (1992).

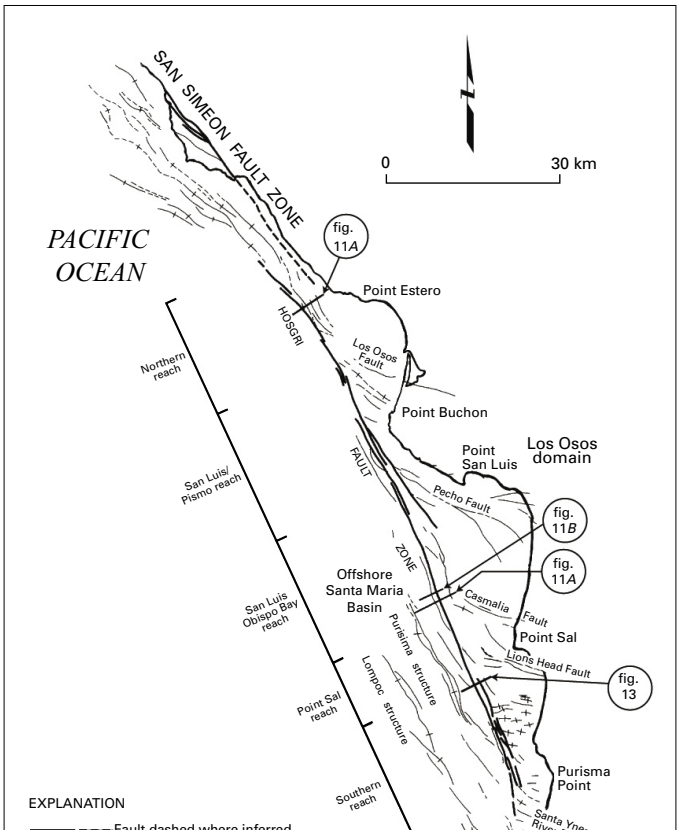


Figure 2. Map of active deformation in the vicinity of the southern San Simeon and Hosgri Fault Zones. The Hosgri Fault Zone separates two regions of contrasting styles and orientations of crustal shortening. Within the offshore Santa Maria Basin west of the Hosgri Fault, active folds (the Purisima and Lompoc structures) are oriented northwest, subparallel to the Hosgri Fault Zone. East of the zone, contractional structures in the Los Osos domain (Lettis and others, this volume) trend oblique to the Hosgri Fault Zone. The Hosgri Fault Zone is divided into five distinct geomorphic reaches based on changes in fault geometry and variations in adjacent structural trends along the fault (Willingham and others, this volume). Shown also are locations of seismic lines displayed in figures 11*A* and *B*, 12, and 13. Seismic lines are labeled according to figure number.

Table 1. Proposed models for sense of slip of the Hosgri Fault Zone.

**Right-slip fault**

- Major displacement: The San Gregorio/Hosgri Fault System is thought to have Neogene displacements on the order of a few tens to more than 100 km (for example, Hall, 1975; Graham and Dickinson, 1978); and Quaternary slip rates of 15 mm/yr (Clark and others, 1984) and 5 to 19 mm/yr (Weber, 1983).

- Minor displacement: In these models, stratigraphic and structural data constrain Neogene displacement on the Hosgri Fault Zone to a total of about 5 km in 5 m.y., yielding a slip rate of about 1 mm/yr (Hamilton and Willingham, 1979; Hamilton, 1982, 1984; Sedlock and Hamilton, 1991). Sorlien and others (1999) estimate a post-Miocene average slip rate of about 2 mm/yr based on restoration of structure-contour mapping of deformed horizons and block rotations along and east of the southern Hosgri Fault. Hanson and Lettis (1994), Hall and others (1994), and PG&E (1988) provide data on displaced Quaternary deposits that indicate a late Quaternary slip rate of 1 to 3 mm/yr for the San Simeon Fault Zone.

**Dip-slip**

- Reverse fault: In this model the Hosgri Fault Zone is interpreted as a steep, east-dipping basin margin reverse fault (Hoskins and Griffiths, 1971).

- Thrust fault: The Hosgri Fault Zone is viewed as one of several listric coastal thrusts that root in an aseismic detachment zone that displaces the San Andreas Fault at depth (Crouch and others, 1984; Crouch and Suppe, 1993).

  Another model of detachment faulting has been proposed by Namson and Davis (1988; 1990). These former detachment faults have been reactivated by Pliocene and younger northeast-southwest shortening (Crouch and others, 1984; Crouch and Bachman, 1987; Namson and Davis, 1990; Crouch and Suppe, 1993).

**Oblique-slip**

- Right normal: The Hosgri Fault is regarded as a complex, extensional (southwest-dipping) Tertiary basin-margin tectonic boundary along which some strike slip movement also probably has occurred (McCulloch, 1987).

- Right reverse: In the current tectonic environment, the Hosgri Fault is interpreted to be a right-oblique-slip fault having a slip rate of about 5 mm/yr (Brown, 1990).

# Previous Investigations

To date, the Hosgri Fault Zone has been interpreted variously as a strike-slip, reverse, thrust, normal, and oblique-slip fault (table 1). This range of interpretations results primarily because the fault bearing this name is a complex zone of deformation that lies entirely offshore where it cannot be directly observed (although its presumed continuation is visible near San Simeon) and because our understanding of the evolution of the Pacific/North American plate boundary continues to develop. In addition, individual investigators typically have relied on only one data set or data from only one location along the fault zone, which has, in turn, led to data-specific or site-specific interpretations of the fault zone. Most investigators, however, generally agree that the zone has a broad range of deformational styles that commonly mask one another and that it is a significant active structure in the contemporary tectonic setting.

Several authors consider the Hosgri Fault Zone to be the southernmost component of a complex system of right-slip faults along the California coast that also includes the San Gregorio, Sur, and San Simeon Faults to the north (fig. 1) (Silver, 1974; Hall, 1975; Graham, 1976; Graham and Dickinson, 1978; Seiders, 1979; Hamilton, 1984; PG&E, 1974, 1975, 1988; Sedlock and Hamilton, 1991). These authors, however, do not agree on the amount, timing, or distribution of large-magnitude, right-slip events on the faults within this system. On the basis of early studies by PG&E and the U.S. Geological Survey (USGS) (Wagner, 1974), PG&E (1974) concluded that the fault zone is a complex extensional basin-margin tectonic boundary along which some strike-slip displacement had occurred. McCulloch (1987) also advocated

the concept of the Hosgri Fault Zone as a Miocene transtensional fault zone. In the 1970s, several authors interpreted that all or some parts of this fault system were the locus of significant Neogene right slip ranging from a total of 90 km to as much as 150 km (Silver, 1974; Hall, 1975; Graham, 1976; Graham and Dickinson, 1978; Clark and others, 1984). In contrast to these estimates, other authors (Hamilton and Willingham, 1977, 1978, 1979; Seiders, 1979; Hamilton, 1984; Sedlock and Hamilton, 1991; Sorlien and others, 1999) have argued for lesser amounts of Neogene displacement on the San Gregorio/Hosgri Fault system or its components and refer to geologic or geomorphic features that limit the amount of cumulative right slip. According to Hamilton (1984) and Sedlock and Hamilton (1991), for example, slip along the San Gregorio/Hosgri Fault system in the past 5 million years has amounted to about 5 km of right-lateral displacement. These authors concluded that the fault system had an earlier history of displacement as part of a late Paleocene "proto-San Andreas" Fault system, which underwent about 150 km of right slip along a combined San Andreas/San Gregorio trace at the north, with the amount of cumulative slip distributed southward on several strands, including about 100 km along a San Simeon/Hosgri strand. Sorlien and others (1999) present a transrotational model for the Santa Maria Basin that indicates a total post-Miocene right-slip displacement of 10.5 km for the southern Hosgri Fault. This includes 7 km of dextral shear from clockwise rotation of blocks east of the Hosgri Fault Zone in addition to 3.5 km of fault slip measured from restored structure contour maps of deformed horizons along the southern Hosgri Fault.

The view of the Hosgri Fault Zone as a fundamental right-slip fault was challenged in the 1980s by several workers who called attention to the significance of crustal shortening in south-central coastal California. Crouch and others (1984), for example, proposed that post-Miocene deformation within central California west of the San Andreas Fault is characterized by a system of listric thrust and reverse faults that splay upward from a gently east-dipping "aseismic detachment zone" that underlies the region at a depth of 10 to 12 km. In this interpretation, the Hosgri Fault is a listric thrust fault with little or no cumulative post-Miocene strike slip. Crouch and others (1984) base their model on (1) the existence of subparallel faults and asymmetric folds; (2) the absence of folds arranged in an en echelon pattern indicative of wrench faulting; and (3) the presence of shallow, east-dipping reflectors on seismic reflection profiles. They concluded that, although some minor strike slip is possible, "the folds and faults, as well as present morphology of the offshore Santa Maria Basin, chiefly reflect post-Miocene northeast-southwest-directed compression" (Crouch and others, 1984, p. 37). More recently, Crouch and Suppe (1993) proposed that the Santa Maria Basin and adjacent regions in central California underwent large-magnitude crustal extension during late Oligocene and early Miocene time. They concluded that many former detachment faults and high-angle normal faults in the hanging wall above the major detachments were reactivated by the Pliocene and younger northeast-southwest shortening.

Namson and Davis (1988) interpreted the Hosgri Fault Zone to be a major thrust fault that has uplifted the southwest flank of the Coast Ranges. On the basis of the construction of regional balanced cross sections, Namson and Davis (1990) subsequently interpreted the fault zone to be a former basin-margin normal fault that has been deformed and rotated into its present eastward-dipping geometry by an underlying thrust fault. In this later model, the fault may have undergone reactivation as a reverse fault during the late Pliocene and Quaternary.

Historical and instrumental seismicity also have been used to interpret the contemporary style of faulting along the San Gregorio/Hosgri Fault system in general, and the Hosgri Fault Zone specifically. Brown (1990), for example, cites earthquake focal mechanisms along the San Simeon Fault Zone reported by Eaton (1984) that show nearly equal components of reverse and strike slip to infer right-oblique slip along the fault zone directly to the south. Brown further uses a lateral slip rate of about 5 mm/yr, estimated from paleoseismic studies along the San Simeon Fault Zone (Weber, 1983; Hanson and others, 1987), and offshore geomorphic and seismic evidence to infer an oblique-slip rate of about 5 mm/yr along the Hosgri Fault Zone. Crouch and others (1984) use reverse focal mechanisms from the offshore Santa Maria Basin to support their interpretation that the fault zone is part of a basin-wide system of listric thrust faults. However, PG&E (1988) and McLaren and Savage (2001) showed that several focal mechanisms from microearthquakes whose epicenters plot directly on the trace of the Hosgri Fault Zone indicate pure right-lateral slip along a northwest-trending focal plane parallel to the fault. Thus, there have been different interpretations of the sense of slip along the Hosgri Fault Zone inferred from historical and instrumental earthquake activity.

# Style and Rate of Late Quaternary Deformation

Characterization of the geometry and contemporary style of faulting along the Hosgri Fault Zone requires an integrated analysis of multiple data sets and several lines of evidence. As discussed in the following sections, our study includes (1) an assessment of the structural evolution of the fault zone during the Tertiary; (2) the kinematics of the regional tectonic setting; (3) the relationship of the fault zone to the onshore San Simeon Fault directly to the northwest; (4) analysis of seismicity data; (5) analysis of geophysical and bathymetric data; and (6) an evaluation of components of slip along the entire fault zone.

## Tertiary Deformational History

The Hosgri Fault Zone evolved through a long succession of recurrent displacements and associated fold deformation during the Cenozoic. This history of deformation encompasses

a variety of tectonic settings that, in turn, have produced a complex pattern of faulting and folding along the length of the fault and in the bordering areas. To provide a framework for evaluating the recent history of the fault, it is important to recognize the inherited deformation and structures produced during earlier tectonic episodes, and to distinguish them from structures related to or reactivated by Quaternary deformation.

The Hosgri Fault Zone probably developed as a major structure during the Paleogene. As described above, right-lateral displacements on the order of 100 to 150 km along parts of the San Gregorio/Hosgri Fault system have been proposed by Hall (1975), Graham and Dickinson (1978), Dickinson and Snyder (1979), Blake and others (1978) and Clark and others (1984). Studies by Seiders (1979), Hamilton (1982, 1984), and Sedlock and Hamilton (1991) indicate that most of this displacement occurred during the Paleogene.

From the late Oligocene through the middle Miocene, the Hosgri Fault Zone was associated with a series of rapidly subsiding basins within a transtensional plate margin system (McCulloch, 1987). Thick sections of Miocene volcanic and pyroclastic rocks of the Obispo Formation and deep marine sediments of the Monterey Formation are present in these basins west of the Hosgri Fault Zone throughout the offshore Santa Maria Basin. These deposits thicken eastward toward the fault and thin abruptly east of it, suggesting that the fault zone formed the eastern structural boundary of these basins. Consequently, the Hosgri Fault Zone appears to have acted in the Miocene as a high-angle, oblique-slip fault having components of both right-slip and down-to-the-west normal displacement.

The middle Miocene episode of transtensional displacement along the Hosgri Fault Zone gave way to transpression in the latest Miocene and early Pliocene. Structures within the zone and bordering areas (plate 1 in Lettis and others, this volume) record a major late Miocene to middle Pliocene episode of crustal shortening (McCulloch, 1987; PG&E, 1988; McIntosh and others, 1991; Meltzer and Levander, 1991; Clark and others, 1991). The onset of this contractional deformation is roughly contemporaneous with the eastward jump of the east Pacific spreading center into the Gulf of California (Curray and Moore, 1984), an increased rate of right-lateral slip on the San Andreas Fault (Crowell, 1962), and a late Miocene pause in the clockwise rotation of the Transverse Ranges (Hornafius and others, 1986). A second episode of crustal shortening normal to the plate margin also is observed throughout the southern Coast Ranges and offshore Santa Maria Basin. This episode appears to be related to an abrupt 11-degree clockwise rotation of the direction of motion of the Pacific plate about 3.9 to 3.4 Ma (Cox and Engebretson, 1985; Pollitz, 1986; Harbert and Cox, 1989).

## Regional Tectonic Setting

The regional tectonic setting of south-central coastal California has been summarized by Sedlock and Hamilton (1991) and Shen and Jackson (1993). Stress (Mount and Suppe, 1987) and geodetic (Shen and Jackson, 1993) measurements indicate that the current motion between the Pacific and North America Plates is oblique convergence (transpression). In general, the Hosgri Fault Zone is subparallel to the orientation of the vector of movement along the North America/Pacific plate margin (DeMets and others, 1990) (fig. 1).

The Hosgri Fault Zone is a fundamental structural boundary that separates two regions of contrasting styles and orientations of crustal shortening (Lettis and others, 1989, this volume). Structural interpretations of offshore seismic reflection data (Crouch and others, 1984; McCulloch, 1987; Clark and others, 1987; Miller and others, 1992; Howie and others, 1993; Willingham and others, this volume); and onshore geologic mapping (Hall, 1973a, Hall 1973b; Hall and others, 1979; Lettis and Hanson, 1992) show that an abrupt change occurs in the trend of late Cenozoic folds and reverse/thrust faults across the Hosgri Fault Zone (fig. 2; plate 1 in Lettis and others, this volume). East of the fault zone, faults and folds within the Los Osos domain (as defined by Lettis and others, this volume) trend west-northwest, oblique to the trend of the fault trace. West of the fault zone, faults and folds within the Santa Maria Basin trend north-northwest, approximately parallel to the zone. Relative displacement across the Hosgri Fault Zone, therefore, is influenced not only by the continued northward movement of the Pacific Plate relative to a “fixed” North American Plate, which gives rise to right shear along the plate margin, but also by northeast-southwest-oriented crustal shortening within the Los Osos domain east of the fault zone, which also results in right shear across the zone (Lettis and others, this volume).

Regionally, the Hosgri Fault Zone is the southern component of a large linear system of strike- slip faults including the San Gregorio, Sur, and San Simeon Faults. These faults define a system of right-stepping structures that extends for more than 400 km from near Point Reyes on the north to Point Pedernales on the south (fig. 1). Detailed geologic studies in the few localities where these faults are exposed onshore document that their predominant style of late Quaternary deformation is right-slip (Weber and Lajoie, 1977, 1979a, 1979b, 1980; Lajoie and others, 1979; Weber and Cotton, 1981; Weber, 1983; Hall, 1991; Hanson and others, 1992; Hanson and Lettis, 1994; Hall and others, 1994). In particular, detailed mapping of offset marine terraces (Hanson and others, 1992; Hanson and Lettis, 1994) and paleoseismic trench studies (Hall and others, 1994) document late Quaternary right-slip at a rate of 1 to 3 mm/yr along the southern San Simeon Fault Zone directly north of the northern end of the Hosgri Fault Zone. These authors also document less than 0.5 mm/yr of up-on- the-west vertical separation across the San Simeon Fault Zone.

## San Simeon/Hosgri Pull-Apart Basin

Given the apparent spatial relationship of the predominant right-lateral San Simeon Fault and the Hosgri Fault Zone, an understanding of the structural association of the

San Simeon Fault to the Hosgri is essential for assessing the style and rate of contemporary deformation along the Hosgri Fault Zone. Detailed analyses of a variety of geophysical and geologic data in the San Simeon Bay to Estero Bay region (fig. 3*A*, *B*) show that the San Simeon and Hosgri Fault Zones are distinct basement-involved faults that terminate in the near-offshore region (Di Silvestro and others, 1990; Lettis and others, 1990; Willingham and others, this volume). Where these faults overlap, they form a 5-km-wide, 15-km-long en echelon right stepover. As shown on figure 3*A*, *B*, the stepover contains a subsiding basin filled with late Tertiary and Quaternary sediments. Faults having normal separation as indicated by stratigraphic relationships both border and extend north-south across the basin.

The normal faults and subsiding basin define a region of localized extension between the San Simeon and Hosgri Fault Zones. The presence of a structural basin bordered by and containing extensional faults in a right en echelon stepover region between two faults, one of which, the San Simeon Fault, is demonstrated to be a right-slip fault, clearly implies that the basin is a tectonic pull-apart structure in a right-releasing stepover.

Kinematic considerations require that right slip be transferred across the pull-apart between the San Simeon and Hosgri Fault Zones, and thus require that the Hosgri Fault

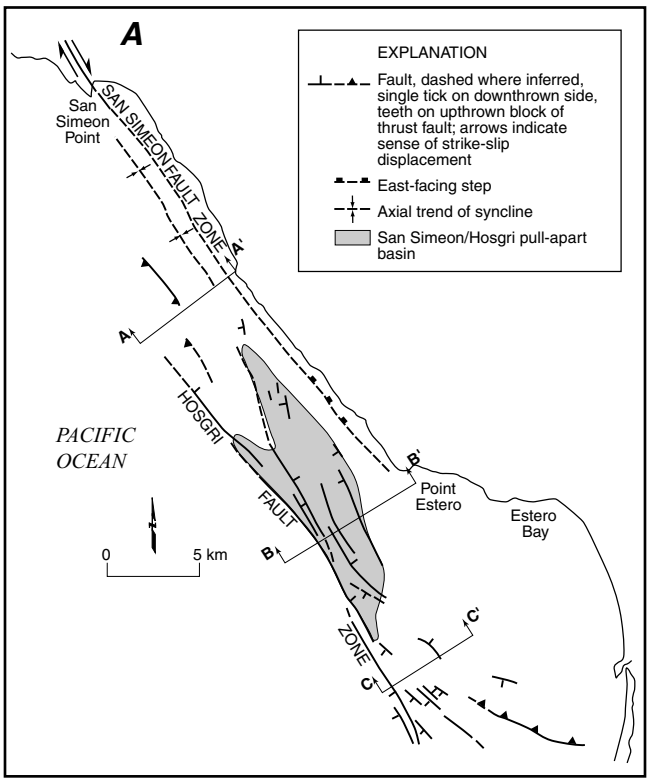


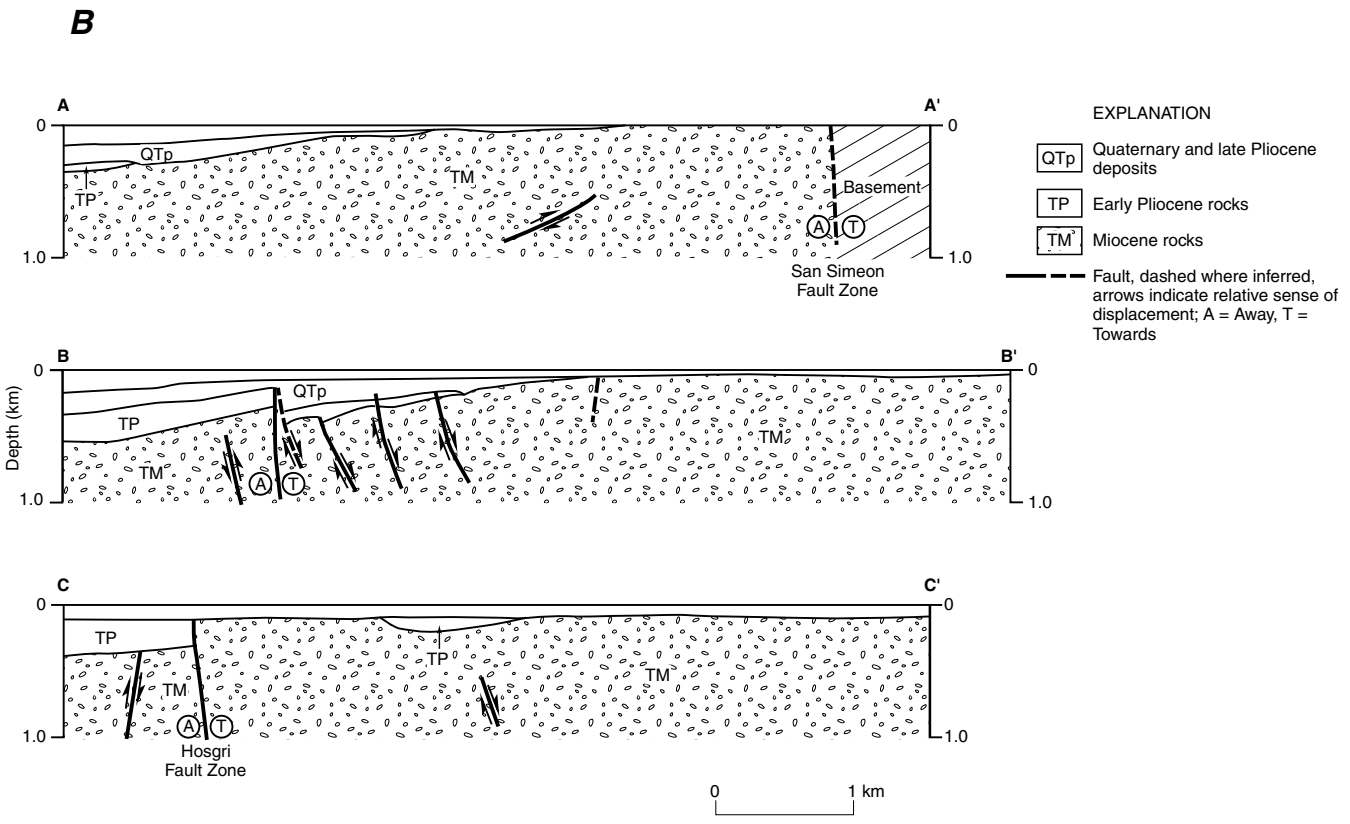


Figure 3. *A*, Map of geologic structures in the San Simeon Bay to Estero Bay region. A subsiding basin bordered by normal faults and containing late Pliocene and younger deposits exists within the stepover region between the Hosgri and San Simeon Fault Zones. *B*, Geologic sections illustrating the stratigraphic and structural relationships north of the San Simeon/Hosgri pull-apart basin (A-A'), through the pull-apart basin (B-B'), and south of the pull-apart basin (C-C'). See figure 3*A* for locations of cross sections.

Zone also be a right-slip fault in the near-coastal region, at least along its northern reach. Lateral slip on the Hosgri is not only consistent with strike-slip faulting regionally, but it also is required to accommodate the contrasting styles of deformation across the fault. Northeast-convergence within the Los Osos domain mechanically requires a component of fault-parallel shortening on the east side of the Hosgri Fault Zone (Lettis and others, this volume), whereas there is no such fault-parallel shortening occurring on the west side of the fault.

## Seismicity

Seismicity patterns based on recent instrumental data analyzed by McLaren and Savage (2001) (fig. 4) also support the observation that the Hosgri Fault Zone is an important boundary separating two regions of contrasting styles and orientations of crustal shortening. The lack of earthquakes and Quaternary structures west of the fault zone north of Point Sal is in marked contrast to the seismicity occurring within the

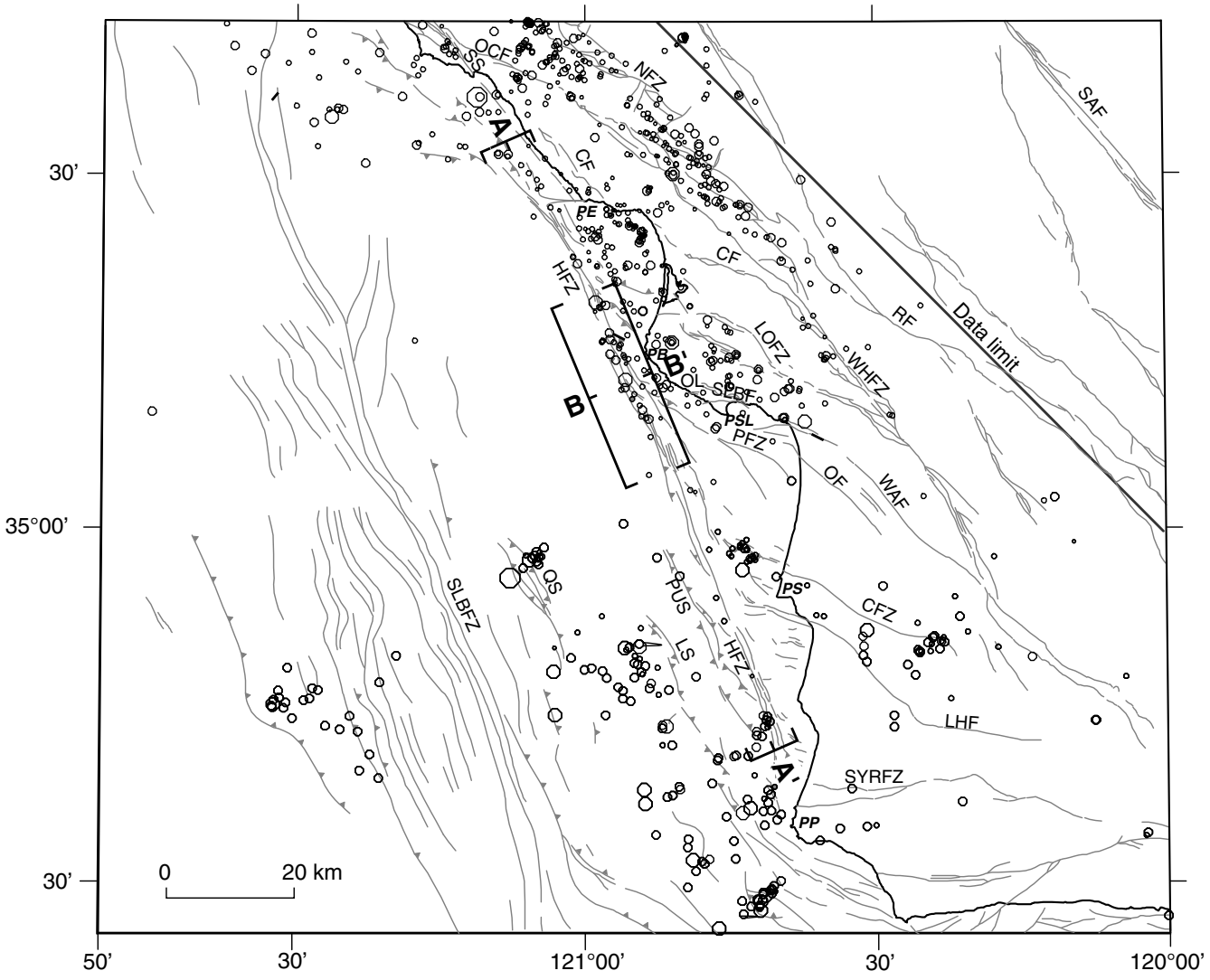


Figure 4. Map showing Quaternary faults, seismicity recorded by the Pacific Gas and Electric (PG&E) Central Coast Seismic Network and the U.S. Geological Survey from October 1987 through January 1997, and the locations of cross sections A-A' and B-B' (fig. 5). Most of the earthquakes are in the 5- to 12-km depth range. The magnitude threshold for detection of onshore and near offshore events (within about 10 km offshore) is about 1.0, whereas for far-offshore areas and near the north and south ends of the network it is about magnitude 1.8. Horizontal and depth uncertainties for onshore and near offshore events are generally less than 1 kilometer and are 1 to about 5 km for far offshore events. Abbreviations: CF=Cambria Fault, CFZ=Casmalia Fault Zone, HFZ=Hosgri Fault Zone, LHF=Lions Head Fault, LOFZ=Los Osos Fault Zone, LS=Lompoc structure, NFZ=Naciemento Fault Zone, OCF=Oceanic Fault, OF=Oceano Fault, OL=Olson Fault, PB=Point Buchon, PE=Point Estero, PFZ=Pecho Fault Zone, PP=Point Pedernale, PS=Point Sal, PSL=Point San Luis, PUS=Purisima structure, QS=Queenie structure, RF=Rinconada Fault, SLBF -San Luis Bay Fault, SLBFZ=Santa Lucia Banks Fault Zone, SS=San Simeon Fault Zone, SYRFZ=Santa Ynez River Fault Zone, WAF=Wilmar Avenue Fault, WHFZ=West Huasna Fault Zone.

uplifting San Luis/Pismo and Casmalia structural blocks to the east (Lettis and others, this volume). This pattern is reversed along the southern part of the Hosgri Fault Zone, where the area of seismic activity lies southwest of the zone in an area characterized by geologic evidence for active faults and folds. In contrast, the region to the east of the fault and south of the Lions Head Fault is relatively quiet.

The November 4, 1927, $M_S$ 7.0 earthquake, which is the largest earthquake recorded in the offshore Santa Maria Basin, occurred near the seismically active region south and west of the Hosgri Fault Zone (PG&E, 1988, fig. 2-27). In the past, the location and tectonic association of this event have been the subjects of considerable debate. Analyses by Byerly (1930), Gawthrop (1978), and Hanks (1979) show that the event probably was located west-southwest of Point Sal at a poorly constrained distance offshore (fig. 1). More recent analyses show that the event had a predominant reverse-slip focal mechanism and occurred about 25 km west of Point Arg uello (Helmberger and others, 1992). This location places the event approximately 40 km southwest of the southern termination of the Hosgri Fault Zone in a zone of active folds and thrust faults along the southern termination of the Santa Lucia Bank Fault (fig. 1).

The establishment of the PG&E Central Coast Seismic Network in 1987 greatly improved earthquake location and focal depth resolution in the near-offshore region. These data can be used to assess seismicity associated with the Hosgri Fault Zone. In earlier studies, very few earthquakes could be confidently associated with the fault zone; small earthquakes at depths ranging from about 4 to 12 km (figs. 4 and 5) are now recognized along the zone. Most of the recent seismicity along the fault has occurred north of Point San Luis (fig. 4) to about 12 km depth (cross-section A-A' of fig. 5).

Focal mechanisms of microearthquakes that plot directly on the trace of the Hosgri Fault Zone primarily show right-slip along a north-northwest-trending fault plane parallel to the zone (fig. 6). Two normal events also have occurred along the zone (fig. 6). One is within the southern part of the San Simeon-Hosgri pull-apart basin, which indicates that this region is currently experiencing extensional strain consistent with the model of an active pull-apart basin in a strike-slip fault zone. The other event, west of Point Buchon, has northwest-trending fault planes and probably occurred on a local secondary structure along the Hosgri Fault Zone.

The distribution of seismicity along the Hosgri Fault Zone also provides an indication of the down-dip geometry of the fault. As shown on cross-section B-B' of fig. 5*B*, microseismicity across the fault zone defines a steeply dipping to vertical plane. Geometric constraints indicated by seismologic data in the Point Sal region, as discussed below, also suggest a steeply dipping to vertical Hosgri Fault.

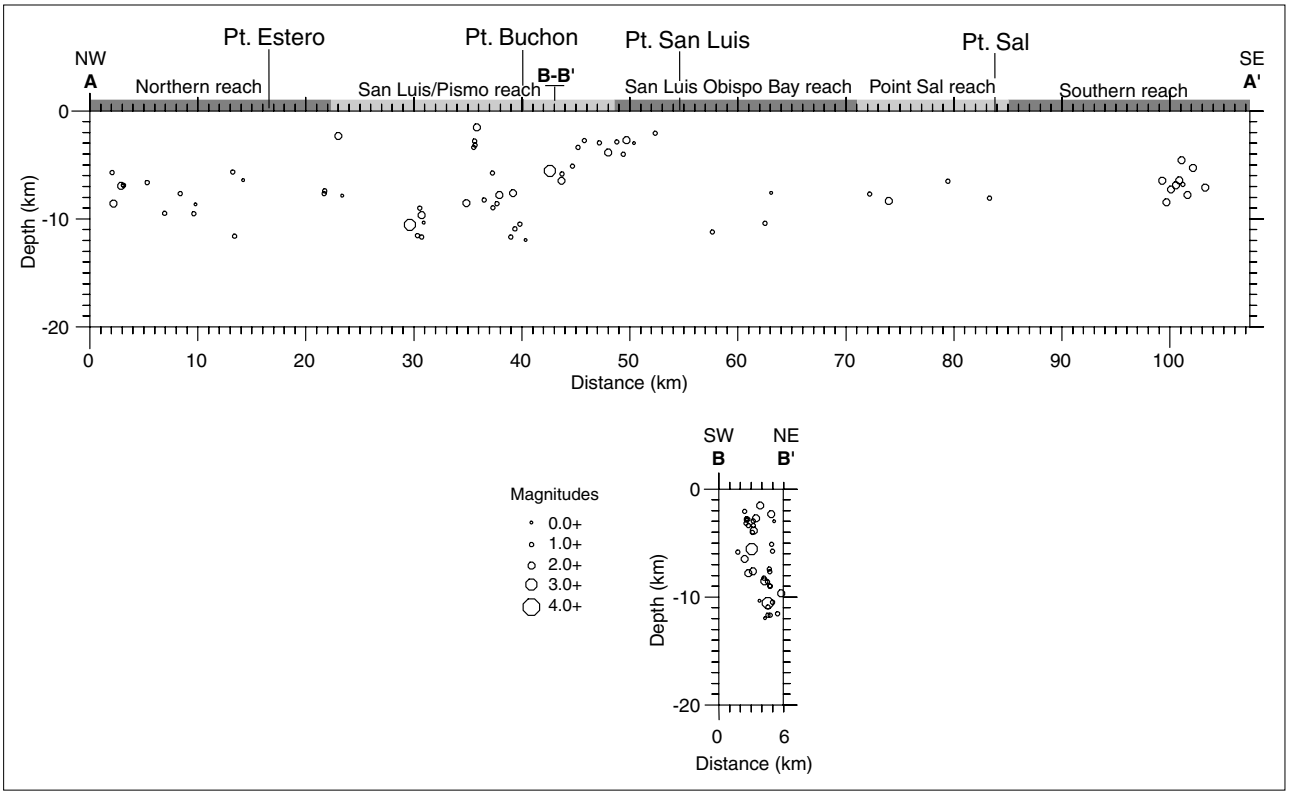


Figure 5. October 1987 through January 1997 earthquakes projected perpendicular to longitudinal cross section A-A' and transverse cross section B-B'along the Hosgri Fault Zone (location and width of the zone of seismicity projected onto cross sections is shown on fig. 4). Geographic locations and reach boundaries are marked.

## 1980 Point Sal Earthquake Sequence

Analysis of the May 29, 1980, Point Sal earthquake (M 5.1) and 1984 aftershock, and the more recent earthquakes recorded between October 1987 and January 1997, provide additional information regarding the down-dip geometry of the Casmalia Fault. The earthquakes occurred in the offshore region near the intersection of the Hosgri and Casmalia Faults (fig. 7). The epicentral locations of the 1980 Point Sal earthquake and a 1984 aftershock (M 3.8) are located approximately 1 km southwest of the surface trace of the Casmalia Fault at a depth of 7 km (fig. 7*A*, *B*, *C*). Focal mechanisms constructed from P-wave first motion data from the 1980 main shock (Eaton, 1984) and the magnitude 3.8 aftershock (McLaren and Savage, 1987) show nearly pure reverse fault planes striking about N70°W and N55°W, respectively, consistent with models of the Casmalia Fault as a southwest-dipping reverse fault (Krammes and Curran, 1959; Crawford, 1971; PG&E, 1988; Lettis and others, this volume). As illustrated on figure 7*B* and 7*C*, most of the recent earthquakes are located at depths of between 5 and 10 km and appear to be associated with a steep (55° to 80°) southwest-dipping Casmalia Fault Zone. Estimated depths for the 1980 event vary between 6 to 9 km—6.5 km (McLaren and Savage, 1987), 7.4 km (this study), and 9.2 km (Eaton, 1984).

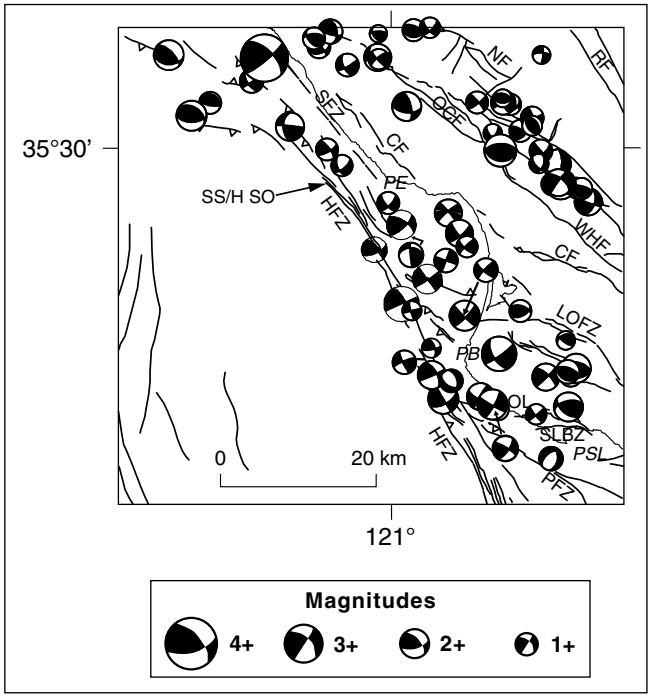


Figure 6. P-wave first motion focal mechanisms for earthquakes recorded from October 1987 through January 1997 (modified from McLaren and Savage, 2001). Mechanisms of earthquakes along the Hosgri Fault Zone north of Point San Luis show predominantly right-lateral strike-slip motion along northwest-trending fault planes parallel to the Hosgri Fault Zone. Strike-slip mechanisms in Estero Bay, south of Point Estero, may be the transfer of strike-slip motion in the stepover region from the Hosgri Fault Zone to the San Simeon Fault Zone. SS/HSO=San Simeon/Hosgri stepover region. See figure 4 caption for other abbreviations.

The distribution of seismicity and the geometry of the Casmalia Fault inferred from the 1980 Point Sal earthquake and 1984 aftershock indirectly show that the Hosgri Fault Zone in this area is a steeply dipping to near-vertical fault and is not consistent with a shallow listric thrust model for the Hosgri Fault as postulated by Crouch and others (1984). The seismicity occurs east of the Hosgri Fault Zone (fig. 7*C*) and defines north-northeast-directed convergence consistent with the orientation and style of deformation within the Los Osos domain (Lettis and others, this volume). The seismicity extends to a depth of 10 km, showing that the Hosgri-Casmalia Fault intersection occurs below 10 km near the base of the seismogenic crust and that the Hosgri Fault is probably steeper than 65 degrees.

## Geophysical Characterization

Because the Hosgri Fault Zone lies offshore along its entire length, geophysical data have been used to characterize its location, length, down-dip geometry, geomorphic expression on the sea floor, amount and timing of slip, and relationship to other structures. Willingham and others (this volume) summarize the geophysical investigations that have been conducted to characterize the zone. In these investigations of the Hosgri Fault Zone and the adjacent offshore Santa Maria Basin, a large number of geophysical data sets were analyzed including the following types of data:

- Potential field data, including the regional aeromagnetic and gravity maps published by McCulloch and Chapman (1977), Rietman and Beyer (1982), and Beyer and McCulloch (1989).
- Common-depth-point (CDP) seismic reflection data. These data provide the primary imagery at the fault zone to depths of 1 to 3 kilometers but do not show the upper few tens of meters of section beneath the sea floor.
- High-resolution seismic reflection data. Depending on the energy source and the local geology, these data image the sea floor and perhaps the upper few meters to few hundred meters of section beneath the sea floor. High resolution data were used to map sea-floor geomorphic features and identify deformation within the most recent sediment layers (fig. 8).

Interpretations of the seismic reflection data across the Hosgri Fault Zone are provided in Willingham and others (this volume). A detailed discussion of the marine seismic data base, bathymetric data, the processing techniques applied to the seismic data, the velocity models used to depth-convert the seismic interpretations, and the techniques used for interpreting stratigraphic and structural relationships from seismic data and their limitations also are provided in Willingham and others (this volume).

On the basis of the geophysical data, we divide the Hosgri Fault Zone into five reaches characterized by distinct variations in strike, down-dip geometry, trace geometry, amount

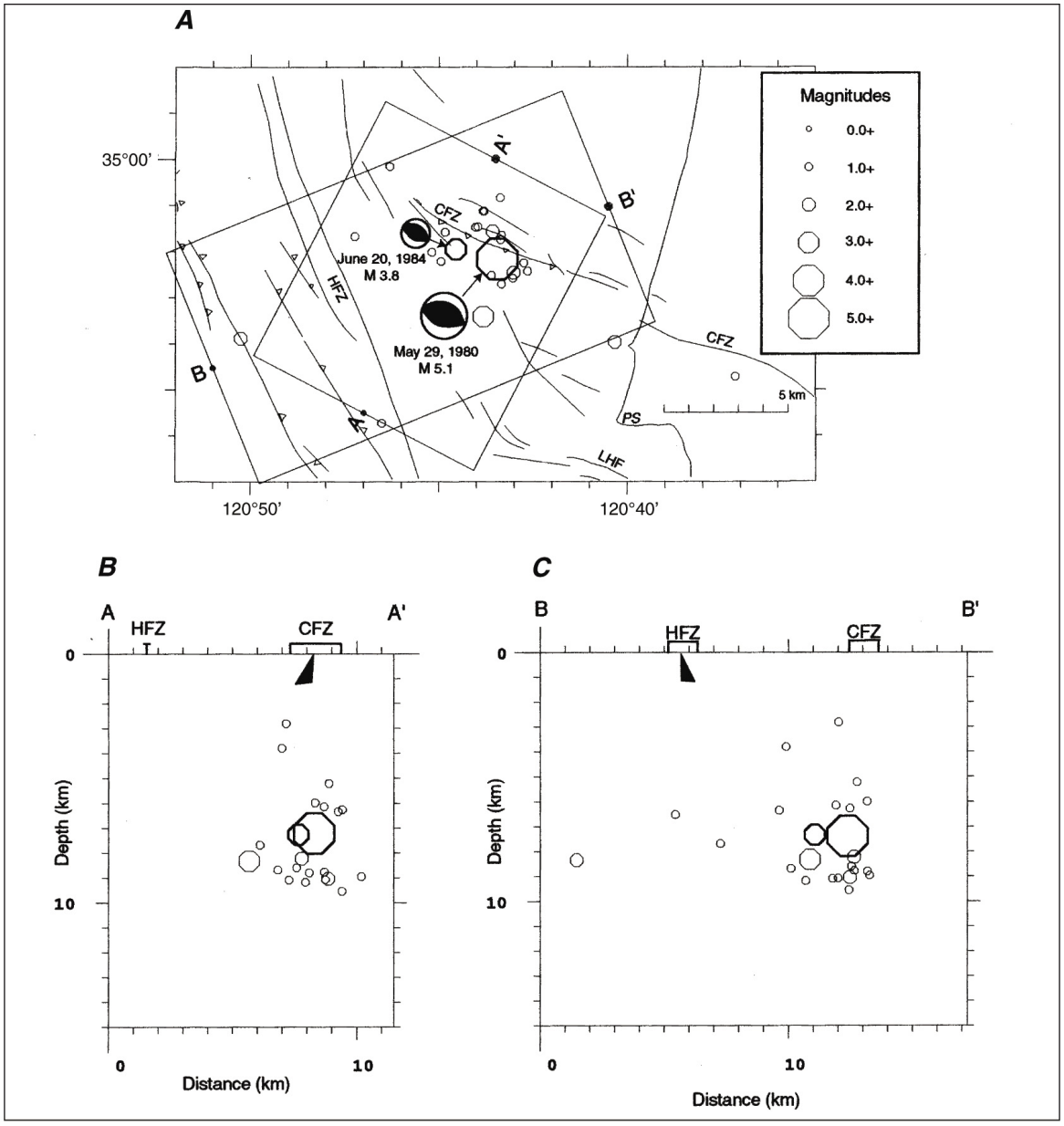


Figure 7. *A*, Map showing the May 29, 1980, M 5.1 Point Sal mainshock and the June 20, 1984, M 3.8 aftershock (heavy outlines) (McLaren and Savage, 1987) and recent earthquakes from October 1987 through January 1997, with locations of cross section A-A', across the Casmalia Fault Zone (CFZ), and B-B', across the Hosgri Fault Zone. The earthquakes were located using a flat layer velocity model and a set of station corrections developed by McLaren and Savage (2001) from recent seismicity data for the southern offshore region, south of the 35th parallel, for input to HYPOINVERSE (Klein, 1989). P-wave first motion focal mechanisms for the 1980 event (Eaton, 1984) and the June 20, 1984, aftershock of magnitude 3.8 (McLaren and Savage, 1987) are shown with arrow to hypocenter symbols. Both focal mechanisms show reverse motion along northwest trending fault planes, subparallel to the Casmalia Fault Zone. Focal mechanisms from our study show similar reverse motion along northwest-trending fault planes. PS, Point Sal; HFZ, Hosgri Fault Zone; LHF, Lions Head Fault. *B*, Cross section A-A' shows most of the earthquakes occurred between 5 and 10 km depth. Earthquakes align against the CFZ at a steeply SW dipping angle, consistent with the dip range (shaded) interpreted by geophysical studies (Willingham and others, this volume). The preferred fault planes from the 1980 and 1984 focal mechanisms are shown and are also consistent with the dip range of 55 ° to 80°. The 7.4 km depth calculated for the 1980 event is shallower than the 9.2 km depth calculated by Eaton (1984) using an iterative process to minimize the root mean square of the solution and deeper than the 6.5 km depth calculated by McLaren and Savage (1987) using the master event technique based on the 1984 aftershock. *C*, Cross section B-B' shows earthquake activity on a transect perpendicular to the HFZ. The range of dips for the HFZ (65°-90°) interpreted by geophysical studies (Willingham and others, this volume) is shown (shaded pattern) beneath the surface projection of the HFZ.

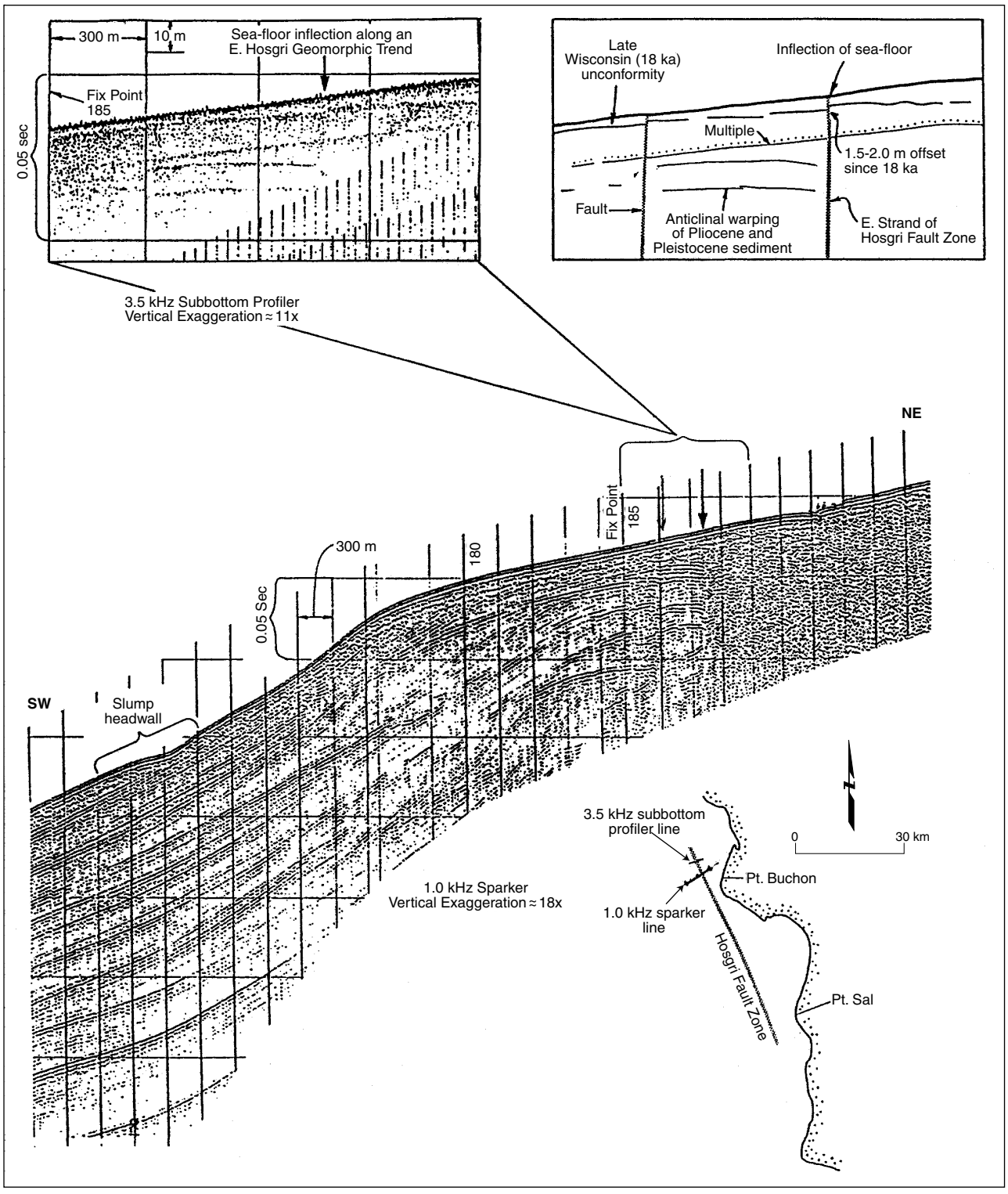


Figure 8. Displacement of the late Wisconsin unconformity and seafloor inflection marking active traces of the Hosgri Fault as imaged on high-resolution seismic data, Fairfield line 224.

and sense of vertical separation, and adjacent structural trends that occur along the fault zone. Each reach borders major onshore structural blocks that abut the fault zone on the east side. Because these blocks typically are bounded by faults that are oblique to the trend of the fault zone, the reach boundaries were generally placed at intersections or projected intersections of these block-bounding faults and the zone (fig. 2). The following reaches have been recognized:

- The Northern reach extends from the northern termination of the fault zone in the San Simeon/Hosgri pull-apart basin south to the intersection with the Los Osos Fault Zone in Morro Bay.
- The San Luis/Pismo reach lies opposite the San Luis/Pismo block and is bounded by the Los Osos Fault Zone on the north and a zone of faults including the Pecho, Wilmar Avenue, Olson, and San Luis Bay Faults on the south.
- The San Luis Obispo Bay reach lies opposite the Santa Maria Valley block.
- The Point Sal reach lies opposite the uplifted block between the Casmalia and Lions Head Faults.
- The Southern reach extends south from the Point Sal reach to the southern termination of the Hosgri Fault Zone offshore from Point Pedernales.

Key observations from the seismic reflection data that we have used to characterize the fault zone complexity, down-dip geometry, sense of slip, and most recent behavior of the Hosgri Fault Zone for each of these reaches are summarized in table 2.

Criteria developed by numerous researchers in academia and the petroleum industry over the past two decades (Bally, 1983) provide a valuable framework for assessing the sense of slip on structures from a suite of seismic reflection data. As described below, comparison of these criteria (see for example, Christie-Blick and Biddle, 1985; Stone, 1986; Zalan, 1987; Withjack and others, 1987; and Harding, 1985, 1989) to the geophysical observations along Hosgri Fault Zone (table 2) argue for contractional strike-slip, rather than predominantly dip-slip or oblique-slip deformation on the fault zone in the contemporary tectonic environment. These authors report that high-angle strike-slip faults are virtually impossible to image directly on seismic reflection data. However, despite this inherent limitation, Christie-Blick and Biddle (1985, p. 2) report that analyses of geophysical data have led to a "growing appreciation for the wide range of structural styles that exist along strike-slip faults, both on the continent and in the ocean basins, and for the processes by which those styles arise." Lynn and Deregowski (1981) show that steeply dipping faults frequently are detectable by indirect means such as a lateral change in reflection character. Lemiszki and Brown ( 1988, p. 665) state that "the complex geology often associated with strike-slip fault zones might also result in severe attenuation, in such a manner as to obscure or mask structural characteristics associated with the deep portions of the faults." In this respect, one should not expect seismic data to image the down-dip geometry of high-angle strike-slip faults in the middle to lower crust. In the following sections, we discuss the key geophysical observations of the Hosgri Fault Zone (table 2) in comparison with worldwide analogs.

## Down-dip Geometry Comparisons

On seismic data, the two high-angle fault strands within the Hosgri Fault Zone are well-constrained in the upper 1 to 3 km to dip from vertical to 60 degrees northeast. At greater depth, the seismic data generally do not provide useful information on down-dip geometry, due to the degradation of data quality in basement rocks and the structural complexity of the fault zone. However, recent analyses involving post- and pre-stack migration of seismic data provide additional constraints on the geometry in the deeper sections (see for example, Shih and Levander, 1989). These studies also conclude that the Hosgri Fault is a high- angle fault.

The seismic data show that the Hosgri Fault Zone is spatially associated with one or more lower-dipping fault strands that are subparallel to and west of the trend of the zone. Many of these faults are truncated by or merge with the Hosgri Fault Zone at shallow depth, whereas others, if projected down their apparent dip, would intersect the fault zone below the depth of imaging. Examples of both cases are shown on plate 3 in Willingham and others (this volume). Most of these low-angle faults are associated with folds, showing that they experienced a significant dip-slip component. In some areas these folds deform the Miocene-early Pliocene unconformity (denoted as the top of Miocene unconformity by Willingham and others, this volume) and the early-late Pliocene unconformity; in other areas, they deform the top of Miocene unconformity but not the early-late Pliocene unconformity. Retrodeformable structural modeling of the folds and underlying dip-slip faults within and along the Hosgri Fault Zone provides constraints on down-dip geometry. The Hosgri Fault, if modeled as a listric, northeast-dipping thrust fault, cannot produce the geometry, spatial distribution, or dimensions of the folds near and within the fault zone (Willingham and others, this volume). This suggests that much of the folding observed adjacent to and west of the Hosgri Fault Zone is not the result of active folding associated with a listric Hosgri Fault Zone at depth. In most areas, these younger folds that deform the early-late Pliocene unconformity are best modeled as positive "flower structures" along a compressional strike-slip fault as discussed in the following section.

## Style of Faulting Comparisons

Analysis of geophysical data (Harding, 1983, 1984, 1985; Harding and others, 1983; Lowell, 1985), as well as geologic data (Sylvester, 1984, 1988), show that most prominent strike-slip faults involve basement and that, in map view, such faults are characterized by a linear or curvilinear principal displacement zone with a variety of associated folds and secondary branching faults confined to a narrow, elongate

zone (fig. 9). The Hosgri Fault Zone displays many of these characteristics of strike-slip fault deformation. The fault zone is linear and is associated with a narrow complex zone of reverse faulting, subparallel folding, and localized extensional deformation (plate 4 in Willingharn and others, this volume). The zone and individual fault strands within the zone are linear at regional scale (greater than 20 km) and curvilinear to linear at local scale (less than 20 km). Fault-trace sinuosity (fault trace length/fault length) is lower than 1.1, similar to other known strike-slip faults (such as the San Andreas and North Anatolian Fault Zones) and different from known reverse or thrust faults (such as the Pleito and San Fernando Faults), where fault-trace sinuosity is greater than 1.2. The low sinuosity independently indicates that the Hosgri Fault dips at a high angle.

The presence of reverse faulting and folding in a narrow, elongate, and linear zone is common along convergent or transpressional strike-slip faults. Characteristics typically observed along convergent strike-slip faults worldwide include reverse faults and low-angle thrust faults, as well as folds arranged both en echelon and parallel to the principal displacement zone (Lowell, 1972; Wilcox and others, 1973; Sylvester and Smith, 1976; Lewis, 1980; Anadon and others, 1985; Mann and others, 1985; Sengor and others, 1985; Steel and others, 1985). Similar features are observed along the Hosgri Fault Zone. As noted by Wilcox and others (1973) and Harding and others (1985), the structural style is affected by even a small component of extension or shortening across the principal displacement zone, circumstances that favor fault-parallel folds rather than en echelon folds (Christie-Blick and Biddle, 1985).

In addition to extensional and contractional deformation on a regional scale, a strike-slip fault also may experience small-scale extensional and contractional deformation along parts of the fault zone as a result of local fault geometry (fig. 10). For example, curvature or abrupt bends along a strike-slip fault, braiding of fault traces within a strike-slip fault system, or en echelon fault traces will produce local areas of extension or contraction along the fault (Crowell, 1974; Woodcock and Fischer, 1986; Reading, 1980). Those local structures occur in restraining and releasing bends (Kadinsky-Cade and Barka, 1989) or en echelon stopovers (Crowell, 1974; Barka and Kadinsky-Cade, 1989; Brown and Sibson, 1989), where contraction and extension, respectively, would be predicted by kinematic models of a strike-slip fault system (see for example, Reading, 1980; Sibson, 1985, 1986; King and Nabelek, 1985; King, 1986; Bilham and King, 1989). These phenomena are common along the Hosgri Fault Zone where small extensional zones characterized by pull-apart structures and/or negative flower structures alternate with reaches along which positive flower structures and fault-parallel folds indicate a component of convergence (Willingham and others, this volume) (fig. 11).

Reversals in the sense of vertical separation both down-dip and along strike also are observed along the fault zone (figs. 12 and 13, table 2). Such reversals are common along strike-slip faults and show lateral offset and juxtapositioning of stratigraphic units at different structural levels.

The diverse styles of faulting along and within the Hosgri Fault Zone imaged on seismic reflection data are typical of strike-slip fault zones, based on examples of several other well-documented strike-slip fault systems worldwide. Indeed, the presence of varied styles of faulting subparallel to and within large strike-slip fault zones is to be expected for several important and commonly occurring reasons:

(1) Many strike-slip fault systems, such as the Hosgri Fault Zone, are oriented oblique to the direction of plate motion, and thus have a component of tensional or compressional stress in addition to the resolved shear stress along the fault zone. The tensional or compressional stress will produce regional extensional or contractional deformation, respectively, along the fault (Sylvester, 1988; Christie-Blick and Biddle, 1985).
(2) Strain partitioning occurs along many regional transpressional strike slip faults (Lettis and Hanson, 1992). Transpressional deformation typically is "partitioned" into nearly pure strike slip on the master fault or principal displacement zone and nearly pure dip slip on adjoining subparallel reverse and thrust faults.
(3) Local bends, en echelon steps, or other changes in local fault geometry will produce localized extensional or contractional deformation along strike-slip faults.
(4) The structural evolution of many strike-slip faults involves the cumulative effects of more than one deformational episode. The imprint of inherited structures and displacements will produce complex, difficult-to-interpret fault geometries, patterns, and sense of displacement (Sylvester, 1988; Christie-Blick and Biddle, 1985). The effects of each prior episode of displacement must be discerned to properly assess the contemporary style of deformation.

All of these phenomena—changing plate motions that have triggered distinct deformational episodes, strain partitioning, and variations in local fault geometries—have played an important role in producing the deformation that we observe along the Hosgri Fault Zone.

## Components of Slip

Evaluating the relative amounts of horizontal and vertical slip along the Hosgri Fault Zone is a key factor in characterizing its style and rate of most recent slip. Faults are historically defined by the rake or direction of displacement in the plane of the fault. In our assessment of sense of slip, we use three classifications of fault types—strike slip, oblique slip, and reverse or dip slip. We define a strike-slip fault as one in which the rake of fault displacement is less than 30 degrees, an oblique-slip fault as one in which the rake is 30

Table 2. Summary descriptions of geomorphic reaches of the Hosgri Fault Zone.

| Reach | Location and Structural blocks[1] | Strike and Length | Geomorphic Expression from Geophysical and Bathymetric Data |
|---|---|---|---|
| Northern | Intersection with Los Osos Fault Zone north to San Simeon Hosgri step-over. | N46°W<br>20 to 22 km | Limited topographic expression; local sea-floor scarps and disruption of late Wisconsin sediment basin |
| San Luis/Pismo | Intersection with Pecho Fault north to intersection with Los Osos Fault Zone. Hosgri Fault Zone forms western boundary of San Luis/Pismo structural block. | N25-30°W<br>20 to 22 km | Discontinuous sea-floor scarps; both traces displace the late Wisconsin unconformity; west trace associated with sea-floor scarps and inflection points. Central zone contains small sediment-filled grabens. East trace forms boundary between deformed bedrock outcrops to the east and sediment-covered basin to the west. |
| San Luis Obispo Bay | Intersection with Casmalia Fault Zone north to intersection with Pecho Fault. Hosgri Fault Zone forms western boundary of Santa Maria Valley structural block. | N15-20°W<br>23 km | Limited topographic expression; sediment-covered over entire reach; west trace and several of the eastern traces locally displace the late Wisconsin unconformity |
| Point Sal | Intersection with southern trace of Lions Head Fault Zone north to intersection with Casmalia Fault Zone. Hosgri Fault Zone forms western boundary of Casmalia structural block. | N20-22°W<br>12 to 14 km | Little to no topographic expression; western trace displaces post-late Wisconsin sediment basin in manner consistent with right slip. Southern 3 km is present at sea-floor. |
| Southern | Southern termination near Point Pedernales north to southern trace of Lion's Head Fault Zone. Hosgri Fault zone forms western margin of Vandenberg/ Lompoc structural block. | N23-25°W changes to N7°W south of Purisima Point.<br>24 to 26 km | Limited to no topographic expression; local sea-floor disruption and deformation of post-late Wisconsin sediments |

[1] Structural blocks are defined in Lettis and others (this volume).

Table 2. Summary descriptions of geomorphic reaches of the Hosgri Fault Zone—Continued.

| Reach | Geophysical Data Observations | Seismicity[2] |
|---|---|---|
| Northern | • One primary fault trace, near-vertical, dips greater than 80°NE<br>• Short west-verging splays merge with near-vertical trace at a depth of 1 to 2 km (one-sided flower structure)<br>• Sense of vertical separation reverses within a single section and along strike<br>• Right-releasing steps have extensional deformation (for example, San Simeon/Hosgri pull-apart basin) | Relatively active; recent seismicity down to 9 km; focal mechanisms indicate right slip on NNW-trending plane |
| San Luis/Pismo | • Two discontinuous vertical to near-vertical faults (east trace and west trace) within a 2- to 3-km-wide zone<br>• Low-angle, west-vergent fault west of western trace<br>• West trace vertical in upper 1 km; dips 65-70°E at depths of 3 to 4 km<br>• East trace dips 70-80°NE<br>• Low-angle fault dips 35-45°NE in near-surface, dip increases to 60°NE at 2 to 3 km<br>• A major change in structural trend occurs across the east (main) trace | Relatively active; recent seismicity down to 12 km; focal mechanisms indicate right slip on NNW-trending plane |
| San Luis Obispo Bay | • Fault zone is complex, with a primary western trace and multiple en echelon eastern traces<br>• Relatively continuous west trace is vertical in upper 1 to 2 km, dips 60-75°NE to a depth of 4 km<br>• Low angle fault dips 30+/-_10° NE, increasing to 60°NE or more at depth<br>• Fault splays diverge upward (flower structures)<br>• Abrupt thinning of Miocene section across fault<br>• Apparent vertical separation of Tertiary and Quaternary strata across main fault trace varies from 0 to 100 m<br>• Right-releasing step-over between west and east traces south of Pecho Fault<br>• Sense of vertical separation reverses within a single section | Relatively quiescent |
| Point Sal | • Two parallel, high-angle faults in a zone 1 km wide<br>• Series of low-angle west-vergent folds (including Purisima structure to the west)<br>• Western high-angle trace is continuous and appears to be near-vertical (70-90°NE) to depths in excess of 2 km<br>• Abrupt thinning of Miocene section across main trace<br>• Fault splays diverge upward (flower structure)<br>• Sense of vertical separation reverses within a single section and along strike<br>• Locally, youngest (Pliocene and Pleistocene) deposits are displaced down on the east | Recent quiescent; a few recent earthquakes were between depths of 6 and 7 km |
| Southern | • Multiple fault traces<br>• West trace continuous south past Purisima Point, discontinuous south of change in trend.<br>• East trace discontinuous, not present south of change in trend<br>• Fault splays diverge upward from western trace (flower structure)<br>• Sense of vertical separation reverses along strike<br>• Fault dips 75°E north of Purisima Point and becomes vertical to the south | Relatively quiescent; a few recent earthquakes were concentrated near Point Pedernales at depths of 5 to 9 km |

[2] Seismicity is discussed in McLaren and Savage (2002).

to 60 degrees, and a reverse or dip-slip fault as one in which the rake is greater than 60 degrees (fig. 14). These definitions, which allow for a continuum of vertical and horizontal components of slip from pure dip slip to pure strike slip, are consistent with definitions used by others (Bonilla and Buchanon, 1970; Slemmons, 1977; Wells and Coppersmith, 1994) to categorize historical surface ruptures for the purpose of evaluating empirical relationships among fault magnitude and various fault parameters. As such, they have been used not only to classify style of faulting on a particular fault zone but also to characterize earthquake behavior.

Assessment of recent slip may be straightforward where the fault is exposed at the surface and its slip vector is shown by a striated fault plane. More challenging cases occur where the fault either is not directly accessible, such as a fault imaged only on seismic reflection profiles or evaluated from borehole data, or where a fault has undergone multiple slip directions over its geologic history. Both conditions apply to the Hosgri Fault Zone, sensu stricto, which lies entirely offshore. The San Simeon Fault Zone, which we consider to be a part of the same system, can be observed on land.

In cases where the rake of a fault cannot be directly measured, the components of horizontal and vertical slip together with the dip of the fault plane can provide an estimate of both the rake and the sense of slip. As shown in figure 15, the cotangent of the rake is the ratio of the strike slip to the dip slip. The amount of strike slip and dip slip implied by the rake can be translated into a ratio of apparent horizontal (H) to apparent vertical (V) separation. Because the apparent vertical separation for a given amount of dip slip is a function of fault dip, the dip of the fault plane is considered in defining the ratios of apparent horizontal to apparent vertical separation that indirectly provide a measure of the rake of displacement in the fault zone. In the case of the Hosgri Fault Zone, geophysical and seismicity data show that the fault is steeply dipping to near vertical to at least a depth of 3 km. Therefore, we present the ratios for each fault class for steeply dipping (60 degrees) to vertical faults on figure 15.

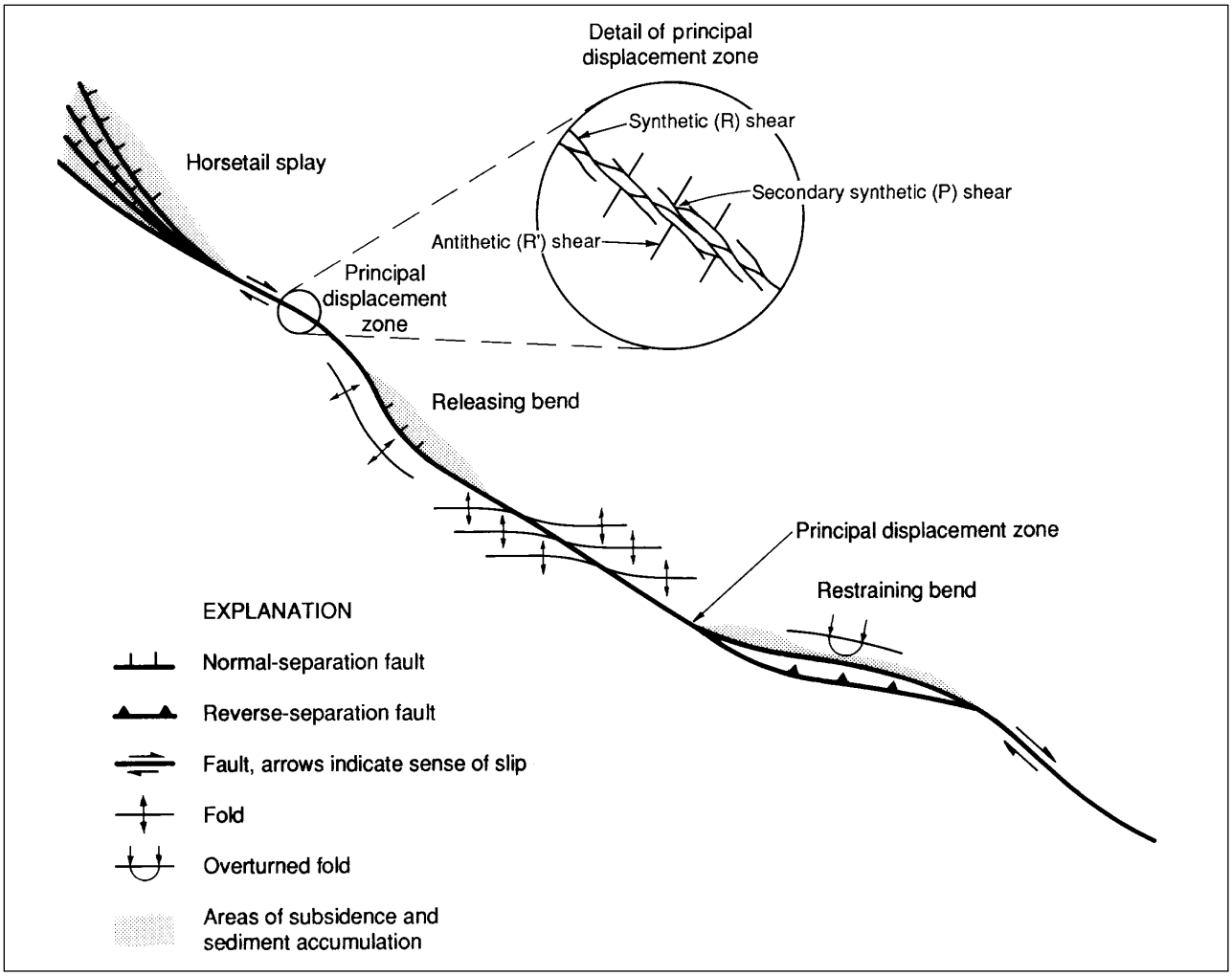


Figure 9. Plan view of idealized right-slip fault showing linear or curvilinear principal displacement zone and associated structures (modified from Christie-Blick and Biddle, 1985).

In the following sections, we discuss constraints on the rates of both horizontal and vertical slip along the fault zone based on analysis of offshore geophysical data, in combination with both onshore and offshore geological observations, and assessment of the regional kinematics and tectonic setting of the fault zone. By examining the rate of vertical separation during defined time intervals, we can differentiate inherited Tertiary deformation from the rate of vertical separation presently occurring across the Hosgri Fault Zone. From this analysis, we can evaluate spatial and temporal variations of ratios of horizontal to vertical slip along the length of the Hosgri Fault and use these ratios to assess its present behavior.

## Lateral Component of Slip

The pattern and style of deformation within the Los Osos domain and the rate and orientation of geodetically determined rates of shortening requires that horizontal slip is occurring on the Hosgri Fault Zone (Lettis and others, this volume). Because there are no recognized marker horizons or features (piercing points) that can be correlated across the Hosgri Fault Zone, horizontal slip during the late Pliocene and Quaternary cannot be measured directly. However, as described earlier, regional tectonic and structural relationships show that horizontal slip is transferred from the San Simeon Fault Zone to the north to the northern Hosgri Fault Zone via the San Simeon/Hosgri pull-apart basin.

Several studies quantify the rate of horizontal slip across the major strands of the San Simeon Fault Zone that is transferred to the Hosgri Fault Zone. Based on an analysis of deflected stream drainages and detailed marine terrace mapping near San Simeon Point, Hanson and Lettis (1994) estimate right-lateral slip rates ranging from 0.7 to 11.2 mm/

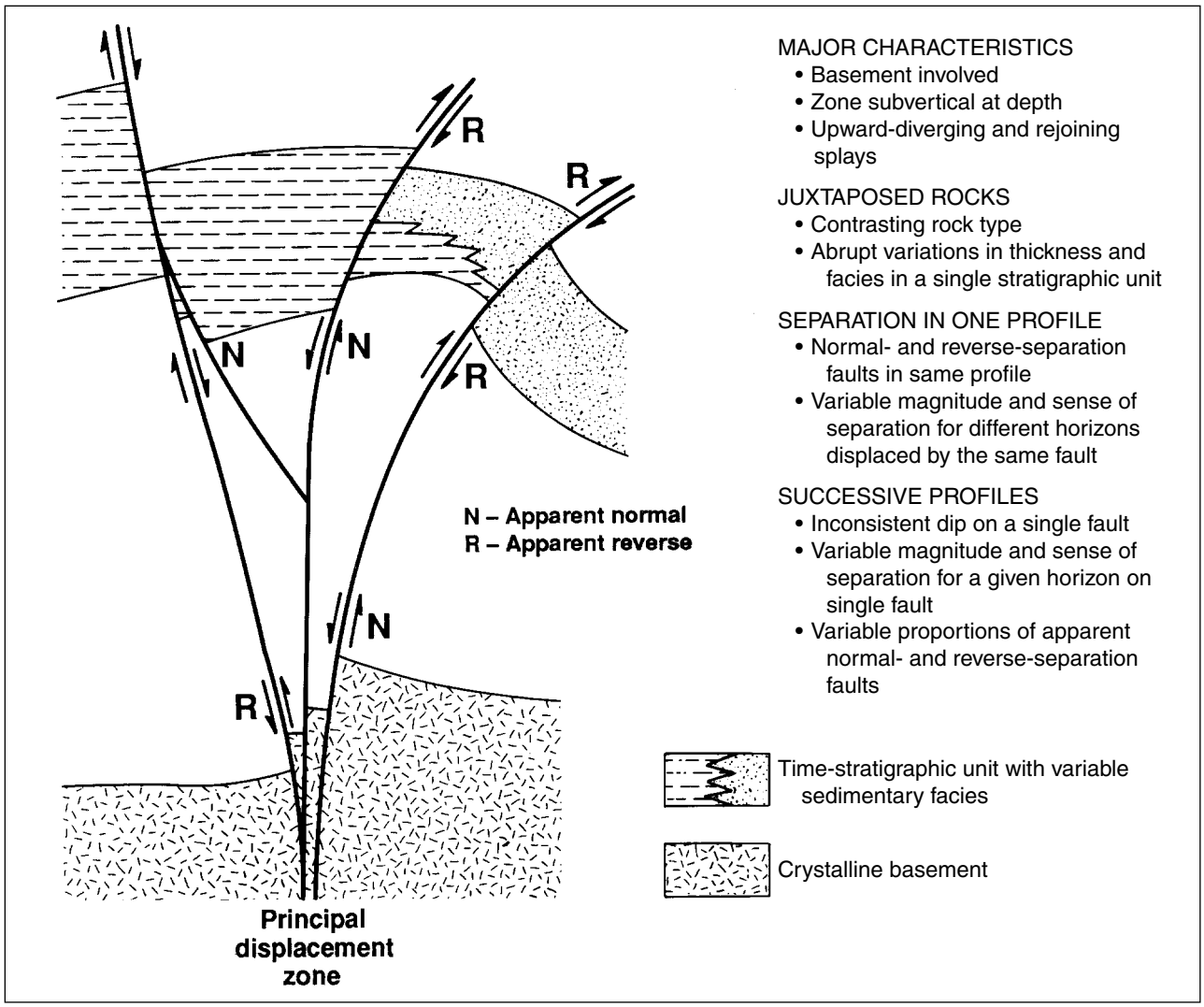


Figure 10. Schematic section of an idealized strike-slip fault showing common stratigraphic and structural characteristics (modified from Christie-Blick and Biddle, 1985).

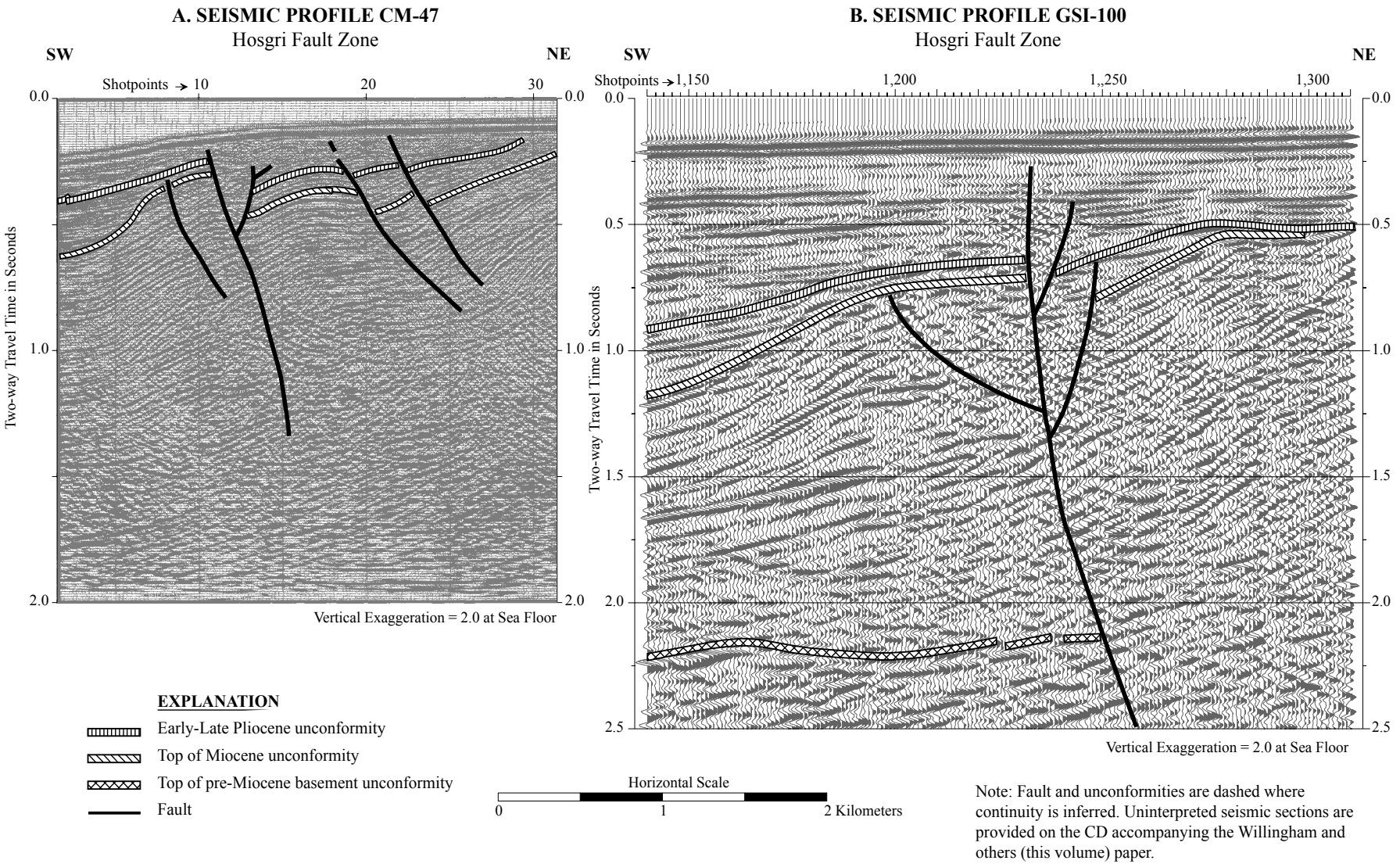


Figure 11. Portions of interpreted migrated-time seismic sections showing normal or negative (profile A) and reverse or positive (profile B) flower structures (upward-diverging splays) along the Hosgri Fault Zone. See figure 2 for location of seismic sections.

yr, with best constrained values of 1 to 3 mm/yr during the past 210,000 yr. Similarly, Hall and others (1994) estimate a minimum Holocene right-lateral slip rate of 1 to 3 mm/yr on the basis of offset fluvial deposits exposed in several trench excavations. We conclude, therefore, that the lateral slip rate along the northern Hosgri Fault Zone ranges from 1 to 3 mm/yr, comparable to slip rates reported along the onshore San Simeon Fault Zone. These rates of horizontal slip are compatible with geodetic rates of crustal shortening in south-central coastal California proposed by Feigl and others (1990) and Shen and Jackson (1993). Based on a model that assumes uniform strain and no rotation, Feigl and others (1990) decompose an integrated rate of deformation into 7 ± 1 mm/yr of contraction along the structural trend oriented N30°E and 3 ± 1 mm/yr of right-lateral shear perpendicular to this axis. Shen and Jackson (1993) show that deep slip along the San Gregorio-Hosgri Fault is about 0 to 4 mm/yr, assuming a locked fault at a depth of 20 km.

## Vertical Component of Slip

Using depth-corrected seismic reflection profiles, we measured the vertical separation of three distinct subhorizontal seismic reflectors, interpreted to be unconformities, across the

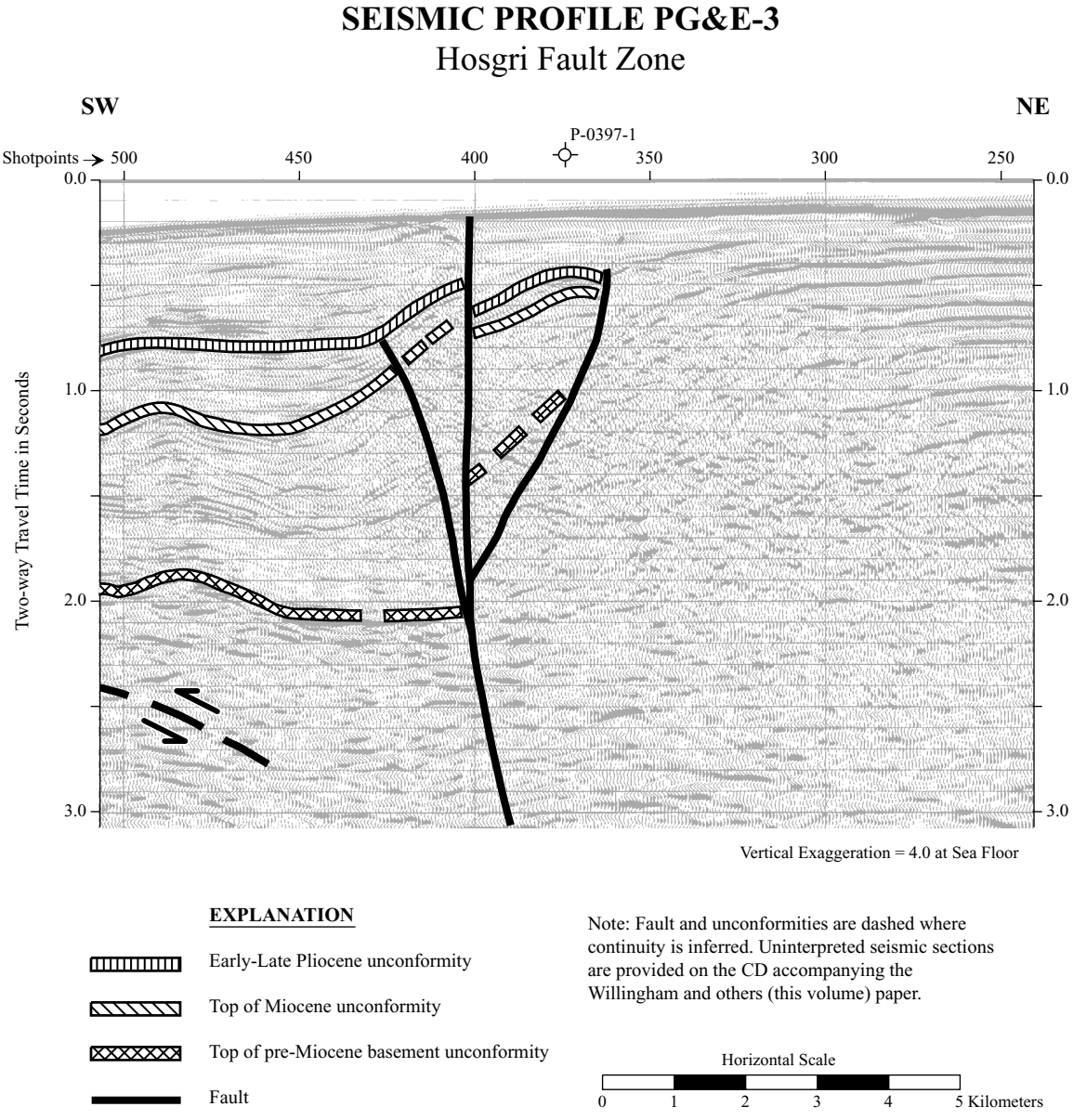


Figure 12. Portion of interpreted migrated-time seismic section showing reversal in sense of slip down-dip on a single trace of the Hosgri Fault. See figure 2 for the location of this seismic line.

entire width of the Hosgri Fault Zone, in order to include both the high- and low-angle components of the fault zone. These unconformities include the top of pre-Miocene basement, top of Miocene, and early-late Pliocene unconformities as denoted by Willingham and others (this volume). Pre-Tertiary rocks, commonly referred to as the "basement complex," include the Franciscan Complex, Jurassic ophiolite, chert and shale, and rocks reported to be Cretaceous in age (Hall, 1982). A discussion of the loop-tie methods used to correlate stratigraphic horizons, the velocity models applied to the time-sections to produce the depth-corrected sections, and the characteristics and ages of the unconformities is provided by Willingham and others (this volume). To estimate the vertical separation due to faulting and (or) folding across the fault zone and to minimize nontectonic factors, we selected inflection points in the unconformities that most likely mark the outer boundaries of the zone of deformation associated with the fault zone. A representative profile showing the technique used to select these points is illustrated in figure 16. As discussed by Willingham and others (this volume), each of these unconformities represents hiatuses that vary in duration from locale to locale within the offshore and onshore Santa Maria Basins. Willingham and others assign the

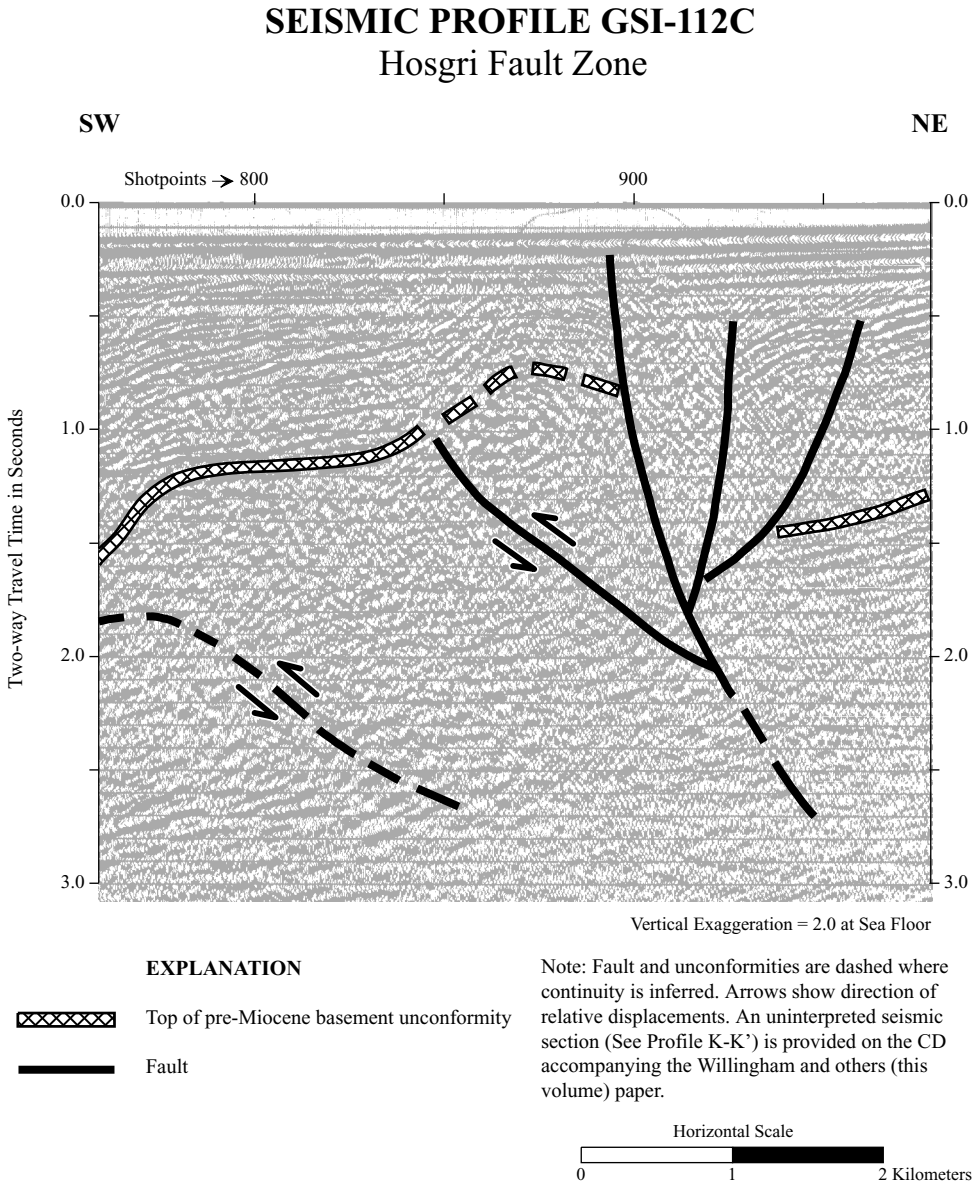


Figure 13. Portion of interpreted migrated-time section showing west-side-up relative displacement of the top of pre-Miocene basement unconformity across the Hosgri Fault. In contrast, the relative sense of vertical separation of the top of pre-Miocene basement unconformity shown in figure 12 is east-side-up. See figure 2 for location of seismic lines.

following age boundaries for these three unconformities—top of pre-Miocene basement unconformity (20 to 17.1 Ma), top of Miocene unconformity (5.3 to 5.1 Ma), and early-late Pliocene unconformity (3.5 to 2.8 Ma). In the calculation of vertical rates of slip based on the deformation of these unconformities, minimum ages for each of the unconformities have been used to provide conservative estimates of the vertical component of slip along the Hosgri Fault Zone.

Table 3 summarizes the measured values of vertical separation across the fault zone of each of the three unconformities along the five reaches of the fault. The measured values include the total vertical separation across the entire fault, including separation due to fold deformation related to the low-angle fault strands within the fault zone, as well as brittle fault deformation and folding associated with the high-angle fault strands. In some areas east of the fault

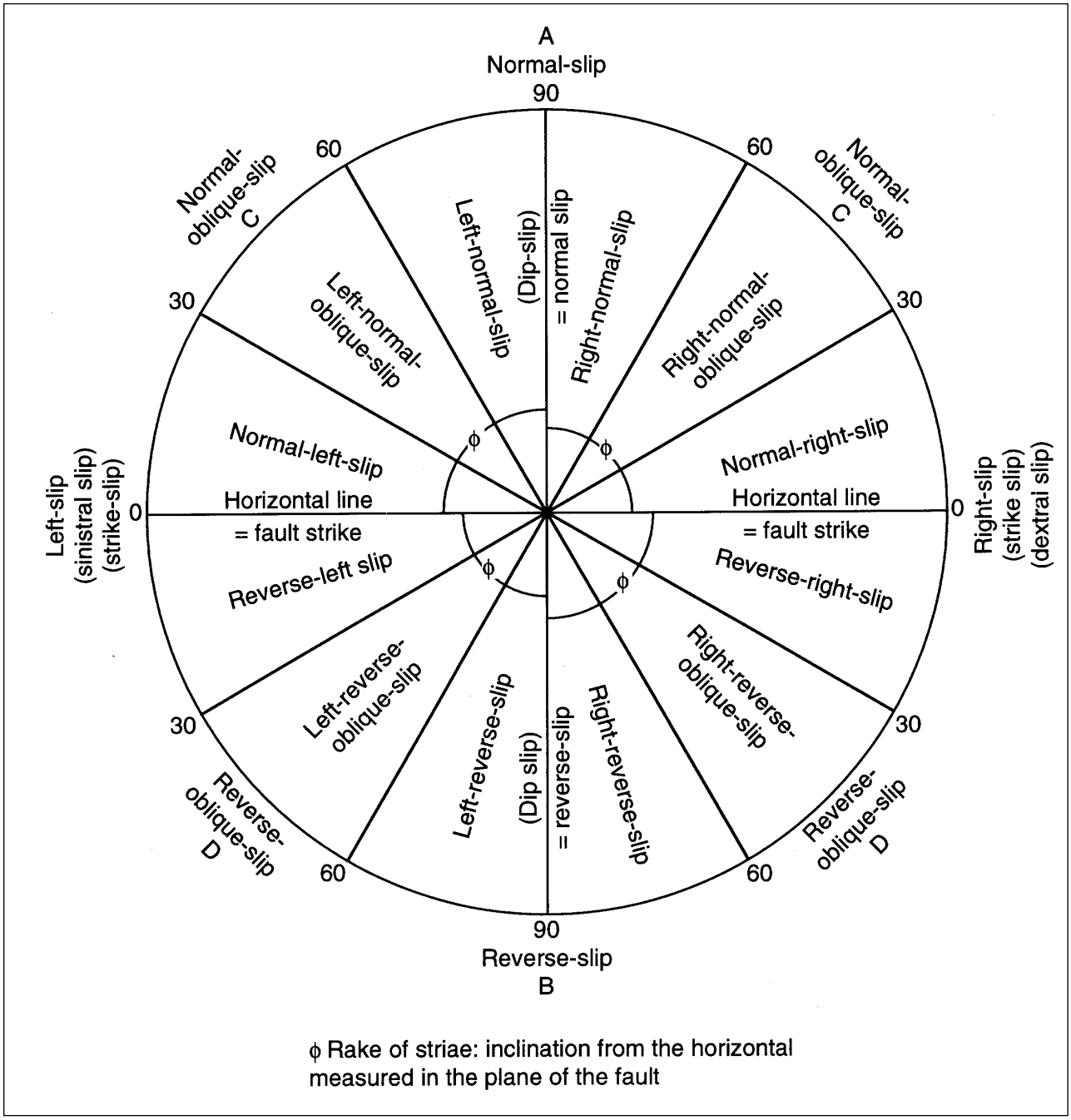


Figure 14. Diagram showing the classification of fault type defined by the rake or direction of displacement in the plane of the fault (from Bonilla and Buchanon, 1970).

zone, uplift has been sufficient to expose basement and older Tertiary bedrock at the present sea floor. Where the younger two unconformities have been eroded, only minimum values of vertical separation can be estimated. In these areas, conservative maximum rates of vertical separation were estimated by directly adding the rate of coastal uplift, based on studies of elevated Pleistocene marine terraces (Hanson and others, 1992, 1994; Clark and Slemmons, 1990), to the maximum values of subsidence based on the altitude of the early-late Pliocene unconformity west of the fault zone. The greater number of values given for the central three reaches of the fault zone (the San Luis/Pismo, San Luis Obispo Bay, and Point Sal reaches) reflects the more complete Tertiary record preserved east of the fault zone along these reaches. On the basis of the measured vertical separation and estimated ages of the top of Miocene and early-late Pliocene unconformities, we also provide in table 3 time-averaged estimates of vertical slip rates. The spatial distribution of these rates of vertical separation for the interval from the late Pliocene to the present is shown on figures 17 and 18.

The estimated vertical slip rates presented in table 3 do not take into account the likelihood that lateral slip has occurred along the Hosgri Fault Zone during these time intervals. The vertical separation of units used to estimate vertical slip rates may be due, in part, to the juxtaposition of irregular or sloping unconformities by lateral slip. However, a comparison of seismic sections on opposite sides of the fault zone that would have been juxtaposed given a right lateral strike-slip rate of 1 to 3 millimeters per year and the ages assigned to each of the unconformities shows that lateral displacement would generally not affect the range of post- top of Miocene and post early-late Pliocene vertical slip rates given in table 3. East of the Hosgri Fault Zone, these unconformities probably attain maximum altitudes within the elevated San Luis/Pismo and Casmalia blocks. West of the fault, these unconformities tilt to the south, subparallel to the Hosgri Fault Zone adjacent to the Northern and San Luis/Pismo and northern San Luis Obispo Bay reaches of the fault (plates 6 and 7, Willingham and others, this volume). Therefore, right-slip along the fault would not increase the apparent vertical separation of these unconformities across the northern half of the fault zone. Consequently, the values of separation that we have measured are a maximum. Correction for lateral slip along the southern San Luis Obispo Bay and Point Sal reaches, however, may result in a higher post early-late Pliocene vertical slip rate than is indicated on table 3. The early-late Pliocene unconformity west of the Hosgri Fault, as imaged on GSI-100 (fig. 11b), is at an altitude of about -712 m (table 3). Assuming that this unconformity has been displaced laterally between 3 to 9 kilometers, a maximum vertical slip rate of 0.42 millimeters per year is calculated by adding a maximum late Pleistocene uplift rate for the Casmalia block (0.17 mm/yr) to the vertical slip rate based on the altitude of the unconformity west of the fault zone in the vicinity of GSI-100 (-712 m ÷ 2.8 million years = 0.25 millimeters per year).

The maximum vertical separation of basement across the fault may exceed the values given in table 3. Based on the altitude of the top of pre-Miocene basement unconformity west of the Hosgri Fault Zone, which ranges from about -1,800 to -2,700 m and the altitude of elevated basement (200 m or greater) in the San Luis/Pismo and Casmalia blocks east of the fault zone, the maximum possible vertical separation of basement juxtaposed laterally across the fault zone may be on the order of 2,800 to 3,000 m. As described earlier, most of the vertical separation of basement occurred during the Miocene and early Pliocene episode of transtensional deformation along the fault zone. Therefore, we can not use the top of pre-Miocene basement or the top of Miocene unconformities to evaluate vertical slip rates in the present tectonic setting.

| Fault Type | Rake angle ϕ, degrees | SS/DS (cotan ϕ) | H:V (dip 90°) | H:V (dip 60°) |
|---|---|---|---|---|
| Strike-slip | <30° | >1.732 | >1.732 | >2 |
| Reverse Oblique | <60° to 30° | >0.577 to 1.732 | >0.577 to 1.732 | >0.67 to 2 |
| Reverse | 90° to 60° | 0 to 0.577 | 0 to 0.577 | 0 to 0.67 |

SS Strike slip (measured in the fault plane)
DS Dip slip (measured in the fault plane)
H Apparent horizontal offset
V Apparent vertical separation

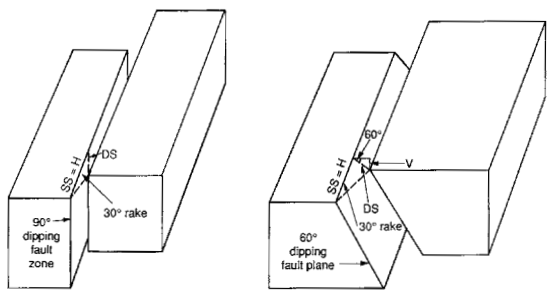


For a 90°-dipping fault plane (rake 30°):

Cotan 30° = SSDS = 1.732
Give DS = VS =1
Then SS = H = 1.732
H:V = 1.732

For a 60°-dipping fault plane (rake 30°):

Given DS = 1, SS = H = 1.732
Then V = sin 60°/DS = 0.866
H:V = 1.732/0.866 = 2

Figure 15. Block diagrams showing relationships between strike-slip (SS), dip-slip (DS), apparent horizontal offset (H), and apparent vertical separation (V). Ratios of apparent horizontal offset and apparent vertical separation can be used to evaluate the style of faulting given the dip of the fault plane. As illustrated in this figure for a fault dipping greater than or equal to 60 degrees, an H:V ratio greater than 2:1 indicates the fault is a strike-slip fault having a rake angle of <30 degrees.

## Ratios of Lateral to Vertical Slip Along the Hosgri Fault Zone

The ratio of horizontal to vertical slip rate is an important criterion for evaluating style of faulting along the Hosgri Fault Zone. The range in the ratio along the fault zone given a lateral slip rate of 1 to 3 mm/yr and a vertical slip rate of 0.1 to

0.42 mm/yr is 2.3:1 to 30:1. Because the fault dips 60 degrees or more, the rake angles of faulting defined by these ratios of horizontal to vertical slip range from 1.6 degree to 24 degrees. These rake angles clearly meet the definition of a strike-slip fault described above. Therefore, although there is a component of dip slip, the Hosgri Fault Zone is behaving predominantly as a strike-slip fault in the contemporary tectonic setting and not as a dip slip or oblique slip fault.

The ratio of horizontal to vertical slip rate is not constant along the fault zone, nor does it vary monotonically from north

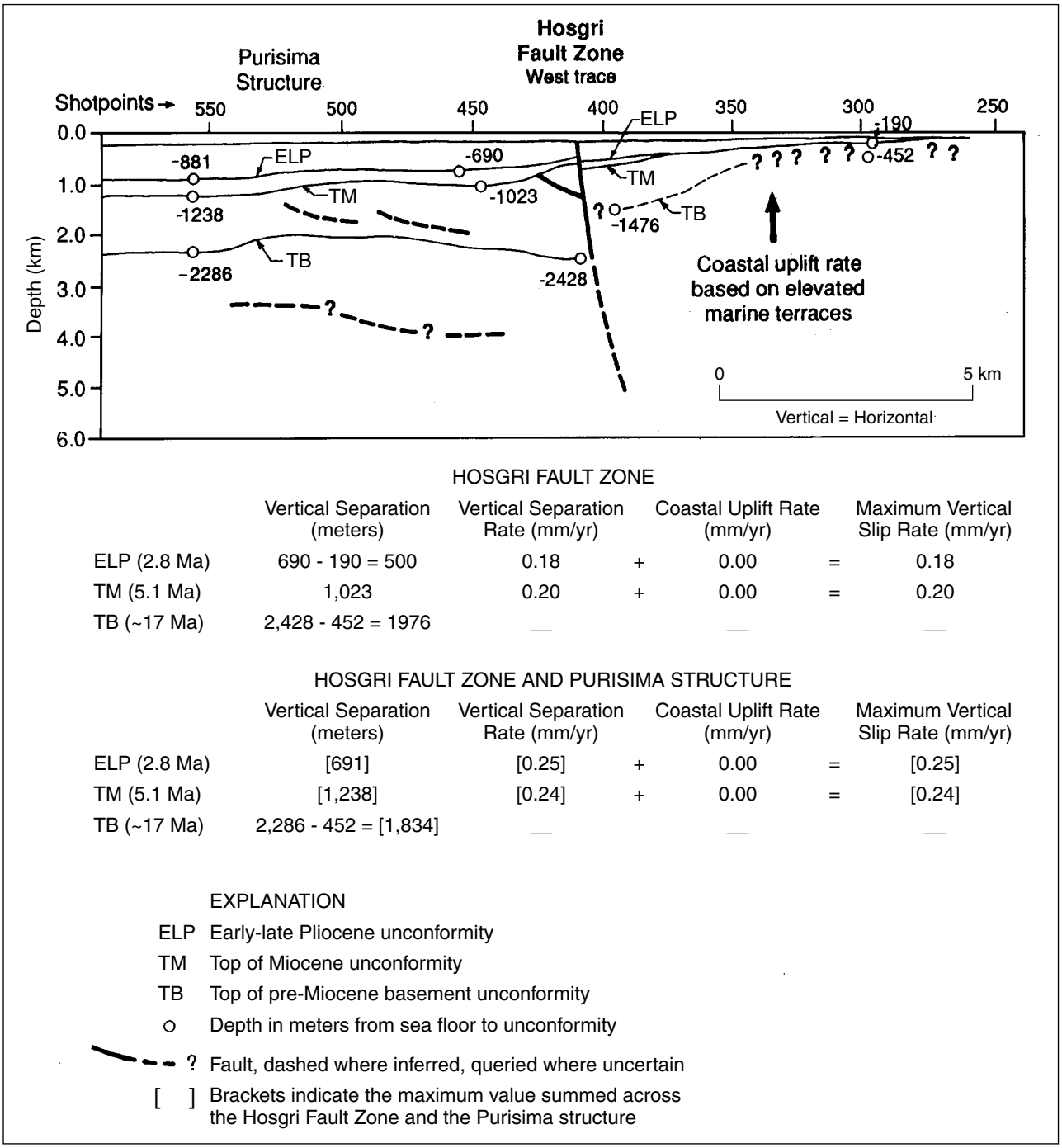


HOSGRI FAULT ZONE

| | Vertical Separation (meters) | Vertical Separation Rate (mm/yr) | | Coastal Uplift Rate (mm/yr) | | Maximum Vertical Slip Rate (mm/yr) |
|---|---|---|---|---|---|---|
| ELP (2.8 Ma) | 690 - 190 = 500 | 0.18 | + | 0.00 | = | 0.18 |
| TM (5.1 Ma) | 1,023 | 0.20 | + | 0.00 | = | 0.20 |
| TB (~17 Ma) | 2,428 - 452 = 1976 | — | | — | | — |

HOSGRI FAULT ZONE AND PURISIMA STRUCTURE

| | Vertical Separation (meters) | Vertical Separation Rate (mm/yr) | | Coastal Uplift Rate (mm/yr) | | Maximum Vertical Slip Rate (mm/yr) |
|---|---|---|---|---|---|---|
| ELP (2.8 Ma) | [691] | [0.25] | + | 0.00 | = | [0.25] |
| TM (5.1 Ma) | [1,238] | [0.24] | + | 0.00 | = | [0.24] |
| TB (~17 Ma) | 2,286 - 452 = [1,834] | — | | — | | — |

EXPLANATION

| | |
|---|---|
| ELP | Early-late Pliocene unconformity |
| TM | Top of Miocene unconformity |
| TB | Top of pre-Miocene basement unconformity |
| o | Depth in meters from sea floor to unconformity |
| ? | Fault, dashed where inferred, queried where uncertain |
| [ ] | Brackets indicate the maximum value summed across the Hosgri Fault Zone and the Purisima structure |

Figure 16. Schematic profile showing technique used to calculate vertical separation. Along the Point Sal and Southern reaches of the Hosgri Fault Zone, the Purisima structure may be considered to be the result of local strain partitioning (Lettis and Hanson, 1992) along the Hosgri Fault Zone, and in this case the vertical structural relief of the structure is included in estimating maximum vertical separation across the Hosgri Fault Zone.

Table 3. Vertical slip rates based on vertical separation of unconformities across the Hosgri Fault Zone.

| SEISMIC LINE | TOTAL VERTICAL SEPARATION (m) | | | | VERTICAL SLIP RATE (mm/yr) | | | | |
|---|---|---|---|---|---|---|---|---|---|
| | TB[1] (~17 Ma) | (~17 to 5.1 Ma) (%)[2] | TM[1,4] (~5.1 Ma) | ELP[1,4] (~2.8 Ma) | Coastal Uplift Rate[3] (mm/yr) | Post TM[1] (5.1 Ma) (mm/yr)[4] | Maximum[5] Post TM[1] (mm/yr) | Post ELP[1] (2.8 Ma) (mm/yr)[4] | Maximum[5, 6] Post ELP[1] (mm/yr) |
| Northern reach | | | | | | | | | |
| CM-51 | I | I | 428 | 119 - 309 | ~0 | 0.08 | 0.08+ | 0.04 - 0.11 | 0.11+ |
| W-76A | ~1922 | (~1335) (~69%) | 642 | 404 | ~0 | 0.13 | 0.13+ | 0.14 | 0.14+ |
| J-113 | ~2113 | ≤1541 (≤72%) | 666 | ≤285 | ~0 | 0.13 | 0.13+ | 0.10 | 0.10+ |
| San Luis/Pismo reach | | | | | | | | | |
| PGE-1 | I | I | 857 | 261 | ≤0.23 | 0.17 | ≤0.40 | 0.09 | 0.32 |
| W-14 | I | I | 710 | 330 | ≤0.23 | 0.14 | ≤0.37 | 0.12 | 0.35 |
| GSI-85 | I | I | 476 - 619 | 285 - 404 | 0.20 - 0.22 | 0.09 - 0.12 | 0.34 | 0.10 - 0.14 | 0.36 |
| GSI-86 | I | I | 690 | 380 | 0.20 | 0.14 | 0.34 | 0.14 | 0.34 |
| GSI-87 | I | I | 880 | 571 | 0.20 | 0.17 | 0.37 | 0.20 | 0.40 (0.26*) |
| San Luis Obispo reach | | | | | | | | | |
| CM-119 | I | I | 881 | 595 | ~0 | 0.17 | 0.17 | 0.21 | 0.21 |
| J-126 | I | I | 1095 | 571 | ~0 | 0.21 | 0.21 | 0.20 | 0.20 |
| GSI-97 | I | I | 1048 | 598 | ~0 | 0.21 | 0.21 | 0.21 | 0.21 |
| GSI-100 Hosgri | I | I | 1119 | 522 | ~0 | 0.22 | 0.22 | 0.19 | 0.19 |
| [Hosgri + Purisima] | I | I | [1238] | [712] | ~0 | [0.24] | [0.24] | [0.25] | [0.25] |
| PGE-3 Hosgri | 1976 | 953 (48%) | 1023 | 500 | ~0 | 0.20 | 0.20+ | 0.18 | 0.18 |
| [Hosgri + Purisima] | [1834] | --- | [1238] | [691] | ~0 | [0.24] | [0.24] | [0.25] | [0.25] |
| Point Sal reach | | | | | | | | | |
| GSI-101 Hosgri | 1715 | ~811 (47%) | 904 | 357 | 0.14 - 0.17 | 0.18 | 0.35 | 0.13 | 0.13 |
| [Hosgri + Purisima] | [1477] | [I] | [1167] | [547] | [0.14 - 0.17] | [0.23] | [0.40] | [0.19] | [0.19] |
| N-204 Hosgri | I | I | 857 | 571 | 0.14 - 0.17 | 0.17 | 0.34 | 0.20 | 0.37 |
| GSI-106 Hosgri | -428[7]- 2095 | -215[7] – 1452 (<0 - 69%) | 643 | 476 | 0.14 - 0.17 | 0.13 | 0.30 | 0.17 | 0.34 |
| [Hosgri + Purisima] | [2000] | [I] | [1143] | [571] | [0.14 - 0.17] | [0.22] | [0.39] | [0.20] | [0.37] |
| Southern reach | | | | | | | | | |
| GSI-112C Hosgri | -732[7] | I | I | I | ~0.14 | I | I | I | I |
| [Hosgri + Purisima] | [756] | [I] | [1122] | [536] | [~0.14] | [0.22] | [0.36] | [0.19] | [0.33] |
| GSI-115 Hosgri | -524[7] | I | I | I | ~0.14 | I | I | I | I |
| [Hosgri + Purisima] | [1501] | [I] | [1024] | [524] | [~0.14] | [0.20] | [0.34] | [0.19] | [0.33] |
| GSI-118 Hosgri | -357[7] | I | I | I | ~0.14 | I | I | I | I |
| [Hosgri + Purisima] | [976] | [I] | [1000] | [570] | [~0.14] | [0.20] | [0.34] | [0.20] | [0.34] |
| GSI-123 Hosgri | 1142 | I | 786 | I | ~0.14 | I | I | I | I |
| [Hosgri + Purisima] | [1261] | [I] | [905] | [476] | [~0.14] | [0.18] | [0.32] | [0.17] | [0.31] |

Notes:

* preferred value based on altitude of exposed basal Squire Member onshore

I, Indeterminate.

[1]TB; top of pre-Miocene basement unconformity, TM; top of Miocene unconformity, ELP; early-late Pliocene unconformity (see Willingham and others, this volume, for a discussion of estimated ages for unconformities).

[2]Percentage of vertical deformation of the top of pre-Miocene basement unconformity that occurred prior to development of the top of Miocene unconformity.

[3]Late Pleistocene uplift rate based on the altitude of the 120,000-year-old marine terrace (Hanson and others, 1992, 1994).

[4]Due to possible erosion of the unconformity east of the Hosgri Fault Zone, the measured vertical separation and resulting vertical slip rate may be minimum values..

[5]Maximum value calculated by adding a maximum coastal uplift rate east of the fault zone to the vertical slip rate based on the difference in the altitude of the unconformity west of the fault zone and the seafloor east of the fault.

[6]Maximum post-early-late Pliocene vertical slip rates shown on figure 17.

[7]Down on the east.

to south along the fault zone. Figure 18 graphically shows the distribution of horizontal and vertical components of slip along the fault and the ratio of slip components along each reach.

The lateral slip of 1 to 3 mm/yr, which is transferred from the San Simeon Fault Zone to the northern part of the Hosgri Fault Zone, probably decreases progressively southward as slip is

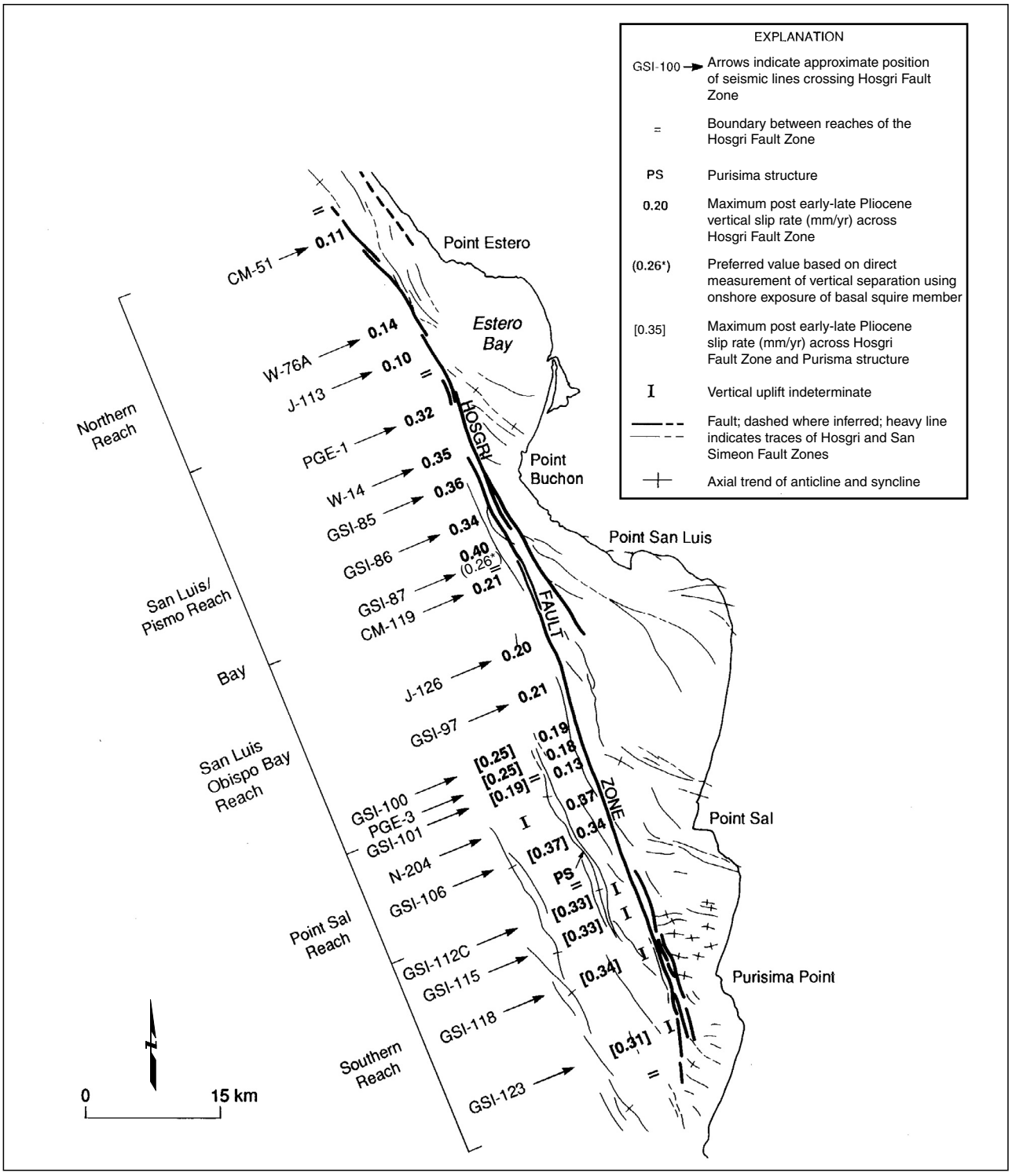


Figure 17. Vertical slip rate estimates based on vertical separation of the early-late Pliocene unconformity as summarized in table 3. Maps showing exact locations of seismic lines, selected seismic profiles, and line interpretations are provided in Willingham and others (this volume).

consumed by crustal shortening along the more westerly trending reverse faults and folds within the Los Osos domain (Lettis and others, this volume). Because faults and folds in the offshore Santa Maria Basin to the west of the Hosgri Fault Zone are either not present or, in the southern part of the region, are subparallel to the fault zone, a similar fault-parallel decay of slip in the offshore does not occur.

For the Los Osos Fault Zone and faults along the southwestern boundary of the San Luis/Pismo block including the Olson, San Luis Bay, and Wilmar Avenue Faults, we use rates of slip determined for these faults on the basis of displaced marine terraces (Lettis and others, 1994). The resolved component of slip tangential to the Hosgri Fault Zone is a maximum of about 0.2 mm/yr for each fault. Similarly,

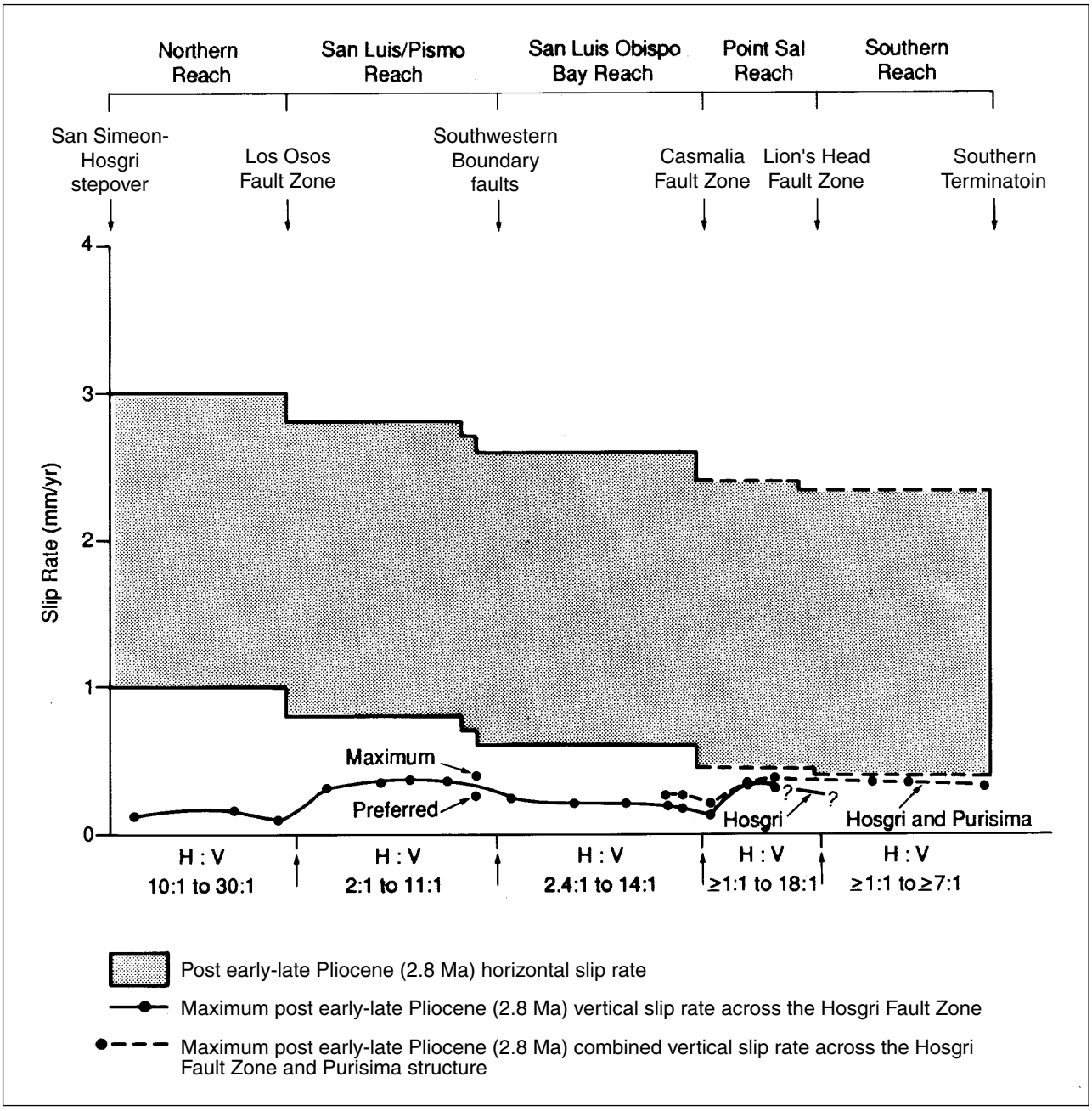


Figure 18. Distribution of lateral and vertical slip rate along the Hosgri Fault Zone, assuming that lateral slip decays southward due to crustal shortening within the Los Osos/Santa Maria domain. Ratios of horizontal slip to vertical slip (H:V) range from 30:1 to 2:1 along the northern three reaches of the fault, indicating that the fault is behaving predominantly as a strike-slip fault. Under extreme scenarios (that is, using minimum estimates of lateral slip and maximum estimates of vertical slip) the fault may become an oblique-slip fault along the Point Sal and Southern reaches.

we assume that these rates are applicable for other faults that intersect the Hosgri Fault Zone, such as the Casmalia and Lions Head Fault Zones. Recent studies by Clark and Slemmons (1990) show that the uplift rate for the Casmalia Hills between the Casmalia and Lions Head Faults is lower than the uplift rate of the San Luis/Pismo block. Based on the estimated vertical separation across these fault zones, the resolved component of slip tangential to the Hosgri Fault Zone is less than 0.2 and 0.05 millimeters per year for the Casmalia and Lions Head Fault Zones, respectively.

As depicted on figure 18, if one assumes a horizontal slip rate of 1 millimeter per year at the northern end of the fault zone, the lower value of the preferred range, the southward decay of horizontal slip by crustal shortening in the Los Osos domain brings the ratio of horizontal to vertical slip to a value of less than 2:1 along the Point Sal and Southern reaches. In these southern parts of the fault zone, the range in ratios of horizontal to vertical slip shows that the fault zone may be either an oblique-slip or a strike-slip fault.

# Conclusions

On the basis of an integrated analysis of a broad spectrum of geological, seismological, geophysical, and tectonic data, we conclude that within the contemporary tectonic setting, the Hosgri Fault Zone is a convergent (or transpressional) dextral strike-slip fault with a late Quaternary slip rate of 1 to 3 mm/yr. Our characterization of the contemporary style and rate of faulting along the Hosgri Fault Zone is summarized as follows.

## Down-dip Geometry

Assessment of down-dip geometry from both high-resolution and common-depth-point seismic reflection data, retrodeformable structural modeling, and seismologic data show a high-angle (60 degrees or greater), down-dip geometry for the primary strands of the Hosgri Fault Zone. Microearthquakes having strike-slip focal mechanisms have occurred along the fault zone near Point Buchon, suggesting a vertical fault to a depth of at least 12 km. The 1980 Point Sal earthquake and aftershock sequence on the Casmalia Fault also constrain the down-dip geometry of the Hosgri Fault Zone to be near-vertical to a depth of approximately 10 km.

## Sense of Slip

The Hosgri Fault Zone is primarily a strike-slip fault with a subordinate component of dip slip in the contemporary tectonic setting. The dip-slip component varies both in cumulative amount and sense (east versus west side up) along strike. We base this conclusion on the following observations and lines of geologic reasoning:

- There is a regional tectonic association and alignment of the Hosgri Fault Zone with the well-documented strike-slip San Gregorio/San Simeon Fault system. The Hosgri Fault Zone aligns with and is nearly identical in structural style and fault zone complexity to these faults. Tectonic and kinematic analyses require that lateral slip continues southward onto the Hosgri Fault Zone. There are no other candidate structures or tectonic explanations that can account for an abrupt termination of lateral slip at the southern end of the San Simeon Fault Zone. The pattern and style of deformation within the Los Osos domain and the rate and orientation of geodetically determined rates of crustal shortening also require that horizontal slip occur along the Hosgri Fault Zone. Interpretations that the Hosgri Fault Zone is predominantly a reverse or oblique-slip fault have severe slip-rate-budget discrepancies and are not consistent with the tectonic setting of south-central coastal California.
- The northern Hosgri Fault Zone is related to the southern San Simeon Fault Zone via the San Simeon/Hosgri pull-apart basin. The presence of a subsiding basin between two large fault zones, one of which (the San Simeon Fault Zone) is a well-documented strike-slip fault, provides strong tectonic and kinematic evidence that the other bounding fault (the Hosgri Fault Zone) is also a strike-slip fault.
- Quantification of components of horizontal and vertical slip along the entire length of the Hosgri Fault Zone indicates ratios of horizontal to vertical slip of 2:1 to 30:1. The quantified rates of vertical slip incorporate the total amount of vertical deformation across the entire fault, including the upper crustal fold deformation related to the low-angle fault strands within the fault zone, as well as brittle fault deformation and folding associated with the high-angle fault strands. Based on the rake angles implied by these horizontal to vertical ratios, together with an estimate of fault dip, the Hosgri Fault Zone is classified as a strike-slip fault along most, if not all, of its length. The uncertainties allow for the possibility that the fault may have oblique slip in the southernmost reaches.
- The Hosgri Fault Zone is comparable in style of deformation to other recognized strike-slip faults based on a review of published criteria to identify and characterize strike-slip faults as they are imaged on seismic reflection data worldwide. Diagnostic characteristics include:

  (1) Reversals in the sense of vertical separation both down dip and along strike of the

fault indicate lateral offset has juxtaposed stratigraphic units at different structural levels.

(2) The presence of local intra-fault-zone pull-apart basins at right-releasing stepovers in the fault trace near Point Sal and Point San Luis indicate right-slip displacement.

(3) Positive and negative flower structures with associated intra-fault-zone anticlinal and synclinal folding are common along the zone. These features are diagnostic of strike-slip faults.

(4) The fault zone and individual fault strands within the zone are linear at regional scale (greater than 20 km) and curvilinear to linear at local scale (less than 20 km). Fault-trace sinuosity is lower than 1.1 and is similar to that along other known strike-slip faults (such as the San Andreas and North Anatolian Fault Zones) and independently indicates a high-angle fault dip. Fault-trace sinuosity is not similar to known reverse or thrust faults (such as the Pleito and San Fernando Faults), where fault-trace sinuosity typically is greater than 1.2.

### Rates of Slip

The net slip rate estimated for the Hosgri Fault is 1 to 3 mm/yr. This estimate includes cumulative lateral and vertical components of slip across the entire fault zone, encompassing high- and low-angle fault strands and structural relief due to folding proximal to the fault zone. The lateral slip of 1 to 3 mm/yr, which is transferred from the San Simeon Fault Zone to the northern part of the Hosgri Fault Zone, probably decreases progressively southward as slip is consumed by crustal shortening along the more westerly trending reverse faults and folds within the Los Osos domain (Lettis and others, this volume). The progressive decrease in the rate of horizontal slip is based on paleoseismic and Quaternary mapping studies conducted along the San Simeon Fault Zone, evaluation of the transfer of slip across the San Simeon/Hosgri pull-apart basin, and consideration of regional tectonics and geodetic rates of crustal shortening in south-central coastal California (Lettis and others, this volume).

Based on the deformation of the early-late Pliocene unconformity, a compressional component of slip also is occurring along the Hosgri Fault Zone in the present tectonic setting. This is consistent with relative plate motions that suggest the Hosgri Fault Zone is presently in a transpressional environment. Post early/late Pliocene vertical slip rates across the Hosgri Fault Zone range from 0.1 to 0.4 millimeters per year, but may be as high as 0.44 millimeters per year if the rate of right-lateral slip along the fault is greater than 1 millimeter per year. These rates are determined from vertical separation of the early-late Pliocene unconformity across the Hosgri Fault Zone combined with uplift of the coast based on elevated Pleistocene marine terraces.

## Acknowledgments

We gratefully acknowledge the contributions of several other individuals who participated in this study. D.H. Hamilton provided significant input to the early synthesis of geological and offshore geophysical data sets to characterize the Hosgri Fault Zone. The geophysical interpretations discussed in this paper reflect the efforts of several geophysicists (including J.D. Rietman, C.R. Willingham, G. Shiller, C.N. Branch, and L.A. Di Silvestro) as noted by Willingham and others (this volume). In particular, we note the work of L.A. DiSilvestro and G. Shiller, who developed the geophysical interpretation of the San Simeon/Hosgri pull-apart basin. Many of the concepts developed during this study resulted from numerous discussions with L.S. Cluff, C.R. Allen, B.A. Bolt, K.J. Coppersmith, and D.B. Slemmons. We thank them for their valuable input and review. We also wish to thank G.A. Thompson and B.M. Page for their helpful reviews. A special thanks to Lloyd Cluff (PG&E) and Margaret Keller (USGS) for their support and encouragement during the entire publication process.

## References

Anadon, P., Cabrera, L., Guimera, J., and Santanach, P., 1985, Paleogene strike-slip deformation and sedimentation along the southeastern margin of the Ebro Basin, *in* Biddle, K. R., and Christie-Blick, N., eds., Strike-slip deformation, basin formation, and sedimentation: Society of Economic Paleontologists and Mineralogists Special Publication No. 37 , p. 303-318.

Bally, A.W., ed., 1983, Seismic expression of structural styles—A picture book and atlas: American Association of Petroleum Geologists Studies in Geology, Series 15, v. 1-3.

Barka, A.A., and Kadinsky-Cade, K., 1989, Effects of restraining stepovers on earthquake rupture, *in* Schwartz, D.P., and Sibson, R.H., eds., Fault segmentation and controls of rupture initiation and termination: U.S. Geological Survey Open-File Report 89-315, p. 67-79

Beyer, L.A., and McCulloch, D.S., 1989, Free-air gravity anomaly map of the offshore Santa Maria Basin: U.S. Geological Survey Open-File Report 89-322, 1 map., scale 1:125,000.

Bilham, R., and King, G., 1989, Slip distribution and oblique segments of the San Andreas Fault, California, observations and theory, *in* Schwartz, D.P. and Sibson, R.H., eds., Fault segmentation and controls of rupture initiation and termination: U.S. Geological Survey Open-File Report 89-315, p. 80-93.

Blake, M.C., Campbell, R.H., Dibblee, T.H., Howell, D.G.,

Nilsen, T.H., Normark, W.R., Vedder, J.G., and Silver, E.A., 1978, Neogene basin formation and hydrocarbon accumulation in relation to the plate tectonic evolution of the San Andreas Fault system, California: American Association of Petroleum Geologists Bulletin, v. 62, p. 344-372.

Bonilla, M.G., and Buchanon, J.M., 1970, Interim report on worldwide historic surface faulting: U.S. Geological Survey Open-file Report 70-34, 32 p.

Brown, N.N., and Sibson, R.H., 1989, Structural geology of the Ocotillo badlands antidilational fault jog, southern California, *in* Schwartz, D.P., and Sibson, R.H., eds., Fault segmentation and controls of rupture initiation and termination: U. S. Geological Survey Open-File Report 89-315, p. 94-109.

Brown, R.D., Jr., 1990, Quarternary deformation, *in* Wallace, R.E., ed., The San Andreas Fault system, California: U.S. Geological Survey Professional Paper 1515, p. 83-114.

Byerly, P., 1930, The California earthquake of November 3, 1927: Bulletin of the Seismological Society of America, v. 68, p. 53-66.

Christie-Blick, N., and Biddle, K.T., 1985, Deformation and basin formation along strike- slip faults, *in* Biddle K.T., and Christie-Blick, N., eds., Strike-slip Deformation, Basin Formation, and Sedimentation: Society of Economic Paleontologists and Mineralogists Special Publication 37, p. 1-34.

Clark, D.G., and Slemmons, D.B., 1990, Late Pleistocene deformation in the Casmalia Hills region, coastal central California: Geological Society of America Abstracts with Program, v. 22, no. 3, p. 14.

Clark, D.H., Hall, N.T., Hamilton, D.H., and Heck, R.G., 1991, Structural analysis of late Neogene deformation in the central offshore Santa Maria Basin, California: Journal of Geophysical Research, v. 96, no. B4, p. 6435-6457.

Clark, J.C., Brabb, E.E., Greene, H.G., and Ross, D.C., 1984, Geology of Point Reyes Peninsula and implications for San Gregorio Fault history, *in* Crouch, J.K., and Bachman, S.B. eds., Tectonics and sedimentation along the California margin: Pacific Section, Society of Economic Paleontologists and Mineralogists, v. 38, p. 67-86.

Clark, D.H., Hamilton, D.H., Hall, N.T., and Heck, R.G., 1987, Timing and style of Neogene deformation within the offshore Santa Maria Basin, California (abs.): EOS, Transactions of the American Geophysical Union, v. 68, no. 44, p. 1365.

Cox, A., and Engebretson, D., 1985, Change in motion of Pacific plate at 5 Myr BP: Nature, v. 313, p. 472-272.

Crawford, F.D., 1971, Petroleum potential of Santa Maria Valley oil field and adjacent parts of the Santa Maria Valley, *in* Cram, I.H., ed., Future petroleum provinces of the United States —their geology and potential: American Association of Petroleum Geologists Memoir 15, p. 316-328.

Crouch, J.K., and Bachman, S.B., 1987, The nature of the offshore Hosgri Fault Zone: Geological Society of America Abstracts with Program, v. 19, p. 369.

Crouch, J.K., Bachman, S.B., and Shay, J.T., 1984, Post-Miocene compressional tectonics along the central California margin, *in* Crouch, J., and Bachman, S.B., eds., Tectonics and sedimentation along the California margin: Pacific Section, Society of Economic Paleontologists and Mineralogists, v. 38, p. 37-54.

Crouch, J.K. and Suppe, J., 1993, Late Cenozoic tectonic evolution of the Los Angeles basin and inner California borderland—a model for core complex-like crustal extension: Geological Society of America Bulletin, v. 105, p. 1415-1434.

Crowell, J.C., 1962, Displacement along the San Andreas Fault, California: Geological Society of America Special Paper 71, 61 p.

Crowell, J.C., 1974, Sedimentation along the San Andreas Fault, *in* Dott, R.H., ed., Modern and ancient geosynclinal sedimentation: Society of Economic Paleontologists and Mineralogists Special Publication, v. 19, p. 292-303.

Cummings, D. and Johnson, T.A., 1994, Shallow geologic structure offshore Point Arguello to Santa Maria River, central California, *in* Alterman, I.B., McMullen, R.B., Cluff, L.S., and Slemmons, D.B., eds., Seismotectonics of the central California Coast Ranges: Geological Society of America Special Paper 292, p. 211-222.

Curray, J.R., and Moore, D.G., 1984, Geologic history of the mouth of the Gulf of California, *in* Crouch, J., and Bachman, S.B., eds., Tectonics and sedimentation along the California margin: Pacific Section, Society of Economic Paleontologists and Mineralogists, v. 38, p. 17-36.

DeMets, C., Gordon, R.G., Argus, D.F., and Stein, S., 1990, Current plate motions: Geophysical Journal International, v. 101, p. 425-478.

Dickinson, W., and Snyder, W., 1979, Geometry of triple junctions related to the San Andreas transform: Journal of Geophysical Research, v. 84, p.561-572.

Di Silvestro, L.A., Hanson, K.L., Lettis, W.R., and Shiller, G.I., 1990, The San Simeon/Hosgri pull-apart basin, south-central coastal California (abs.): EOS, Transactions of the American Geophysical Union, v. 71, no. 43, p. 1632.

Eaton, J. 1984, Focal mechanisms of nearshore earthquakes between Santa Barbara and Monterey, California: U.S. Geological Survey Open-File Report 84-477.

Feigl, K.L., King, R.W., and Jordan, T.H., 1990, Geodetic measurement of tectonic deformation in the Santa Maria fold and thrust belt, California: Journal of Geophysical Research, v. 95, no. B2, p. 2679-2699.

Gawthrop, W.H., 1978, Seismicity and tectonics of the Central California coastal region; *in* Silver, E.A. and Normark, W.R., eds., San Gregorio-Hosgri Fault Zone, California: California Division of Mines and Geology Special Report 137, p. 45-46.

Graham, S.A., 1976, Tertiary sedimentary tectonics of the central Salinan block of California: Palo Alto, California, Stanford University, unpub. Ph.D. dissertation, 510 p.

Graham, S.A., and Dickinson, W.R., 1978, Evidence for 115 kilometers of right slip on the Gregorio-Hosgri Fault trend:

Science, v. 199, p. 179-81.
Hall, C.A., Jr., 1973a, Geologic map of the Arroyo Grande quadrangle, California: California Division of Mines and Geology, Map Sheet 24, scale 1:48,000.
Hall, C.A., Jr., 1973b, Geologic map of the Morro Bay South and Port San Luis quadrangles, San Luis Obispo County, California: U.S. Geological Survey Miscellaneous Field Studies Map MF- 511, scale 1:24,000.
Hall, C.A., Jr., 1975, San Simeon-Hosgri Fault system, coastal California; economic and environmental implications: Science, v. 190, no. 4221, p. 1291-1294.
Hall, C.A., Jr., 1982, Pre-Monterey subcrop and structure contour maps, western San Luis Obispo and Santa Barbara counties, South-central California: U.S. Geological Survey Miscellaneous Field Studies Map MF-1384, 6 sheets, scale 1:62,500.
Hall, C.A., Jr., 1991, Geology of the Point Sur-Lopez Point region, Coast Ranges, California; a part of the Southern California allochthon: Geological Society of America Special Paper 226, 44 p.
Hall, C.A., Jr., Ernest W.G., Prior S.W., and Wiese S.W., 1979, Geologic map of the San Luis Obispo-San Simeon Region, California: U.S. Geological Survey Miscellaneous Investigations Series, Map 1-1097, Scale 1:48,000.
Hall, N.T., Hunt, T.D., and Vaughn, P., 1994, Holocene behavior of the San Simeon Fault Zone, south-central coastal California, *in* Alterman, I.B., McMullen, R.B., Cluff, L.S., and Slemmons, D.B., eds., Seismotectonics of the central California Coast Ranges: Geological Society of America Special Paper 292, p. 167-190.
Hamilton, D.H. 1982, The proto-San Andreas Fault and the early history of the Rinconada, Nacimiento, and San Gregorio-Hosgri Faults of coastal central California (abs.): Geological Society of America Abstracts with Program, v. 63, p. 1124.
Hamilton, D.H., 1984, The tectonic boundary of coastal Central California: Palo Alto, California, Stanford University, Ph.D. dissertation, 290 p.
Hamilton, D.H., and Willingham, C.R., 1977, Hosgri Fault Zone: structure, amount of displacement, and relationship to structures of the western Transverse Ranges (abs.): Geological Society of America Abstracts with Program, v. 9, no. 4, p. 429.
Hamilton, D.H., and Willingham, C.R., 1978, Evidence for a maximum of 20 km of Neogene right slip along the San Gregorio Fault Zone of central California (abs.): Transactions, American Geophysical Union, v. 59, no.12, p. 1210.
Hamilton, D.H., and Willingham, C.R., 1979, The coastal boundary zone of central California (abs.): Geological Society of America, Abstracts with Program, Cordilleran Section Meeting, v. 11, no. 3, p. 81.
Hanks, T.C., 1979, The Lompoc, California, earthquake (November 4, 1927; M=7.3) and its aftershocks: Bulletin of the Seismological Society of America, v. 69, p. 451-462.
Hanson, K.L., and Lettis, W.R., 1994, Estimated Pleistocene slip rate for the San Simeon Fault Zone, south-central coastal California, *in* Alterman, I.B., McMullen, R.B., Cluff, L.S., and Slemmons, D.B., eds., Seismotectonics of the central California Coast Ranges: Geological Society of America Special Paper 292, p. 133-150.
Hanson, K.L., Lettis, W.R., and Mezger, L., 1987, Late Pleistocene deformation along the San Simeon Fault Zone near San Simeon, California (abs.): Geological Society of America Abstracts with Programs, Cordilleran Section, v. 19, no. 6, p. 386.
Hanson, K.L., Lettis, W.R., Wesling, J.R., Kelson, K.I, and Mezger, L., 1992, Quaternary marine terraces, south-central coastal California—implications for crustal deformation and coastal evolution, *in* Fletcher, C.H., and Wehmiller, J.F., eds., Quaternary coasts of the United States: marine and lacustrine systems: Society for Sedimentary Geology Special Publication No. 48, p. 323-332.
Hanson, K.L., Wesling, J.R., Lettis, W.R., Kelson, K.I., and Mezger, L., 1994, Correlation, ages, and uplift rates of Quaternary marine terraces, South-central coastal California, *in* Alterman, I.B., McMullen, R.B., Cluff, L.S., and Slemmons, D.B., eds., Seismotectonics of the central California Coast Ranges: Geological Society of America Special Paper 292, p.45-72.
Harbert, W., and Cox, A., 1989, Late Neogene motion of the Pacific plate: Journal of Geophysical Research, v. 94, p. 3052-3064.
Harding, T.P., 1983, Divergent wrench fault and negative flower structure, Andaman Sea, *in* Bally, A.W., ed., Seismic Expression of Structural Styles-A Picture and Work Atlas: American Association of Petroleum Geologists Studies in Geology, series 15, v. 3, p. 4.2-1 -4.2-8.
Harding, T.P., 1984, Graben hydrocarbon occurrences and structural style: American Association of Petroleum Geologists Bulletin, v. 68, p. 333-362.
Harding, T.P., 1985, Seismic characteristics and identification of negative flower structures, positive flower structures, and positive structural inversion: American Association of Petroleum Geologists Bulletin, v. 69, p. 582-600.
Harding, T.P., 1989, Criteria and pitfalls in identification of wrench faults from exploration data (abs.): Program, 64th Annual Meeting, Pacific Section, American Association of Petroleum Geologists/Society for Sedimentary Geology, p. 31.
Harding, T.P., Gregory, R.F., and Stephens, L.H., 1983, Convergent wrench fault and positive flower structure, Ardmore basin, Oklahoma, in Bally, A.W., ed., Seismic expres sion of structural styles—A picture and work atlas: American Association of Petroleum Geologists Studies in Geology, series 15, v. 3, p. 4.2-13 -4.2-17.
Harding, T.P., Vierbuchen, R.C., and Christie-Blick, N., 1985, Structural styles, plate-tectonic settings, and hydrocarbon traps of divergent (transtensional) wrench faults, *in* Biddle, K.R., and Christie-Blick, N., eds., Strike-slip Deformation, Basin Formation, and Sedimentation: Society of Economic Paleontologists and Mineralogists Special Publication No. 37 , p. 51- 77.

Helmberger, D.V., Somerville, P.G., and Garnero, E., 1992, The location and source parameters of the Lompoc, California, earthquake of 4 November 1927: Bulletin of the Seismological Society of America, v. 82, no. 4, p. 1678-1709.

Hornafius, S.J., Luyendyk, B.P., Terres, R.R., and Kamerling, M.J., 1986, Timing and extent of Neogene tectonic rotation in the western Transverse Ranges, California: Geological Society of America Bulletin, v. 97, p. 1476-1487.

Howie, J.M., Miller, K.C. and Savage, W.U., 1993, Integrated crustal structure across the south central California margin; Santa Lucia escarpment to the San Andreas Fault: Journal of Geophysical Research, v. 98, p. 8173-8196.

Hoskins, E.G. and Griffiths, J.R., 1971, Hydrocarbon potential of northern and central California offshore, *in* Cram, I.H., ed., Future petroleum provinces of the United States their geology and potential: American Association of Petroleum Geologists Memoir 15, p. 212-228.

Jennings, C.W., 1975, Fault map of California with locations of volcanoes, thermal springs and thermal wells: California Division of Mines and Geology, 1 map, scale 1:750,000.

Kadinsky-Cade, K., and Barka, A.A., 1989, Effects of restraining bends on the rupture of strike-slip earthquakes, *in* Schwartz, D.P, and Sibson, R.H., eds., Fault segmentation and controls of rupture initiation and termination: U.S. Geological Survey Open File Report 89-315, p. 181-192.

King, G.C.P., 1986, Speculations on the geometry of the initiation and termination processes of earthquake rupture and its relation to morphology and geological structure: Pure and Applied Geophysics, v. 124, p. 567-585.

King, G.C.P., and Nabelek, J., 1985, The role of bends in faults in the initiation and termination of earthquake rupture: Science, v. 228, p. 984-987.

Klein, F.W., 1989, User's Guide to HYPOINVERSE, a program for VAX computers to solve for earthquake locations and magnitudes: U.S. Geological Survey Open-File Report, 89-314, 58 p.

Krammes, K.F., and Curran, J.F., 1959, Correlation section across Santa Maria Basin: American Association of Petroleum Geologists (Pacific Section), Correlation Section 12, 1 sheet.

Lajoie, K.R., Weber, G.E., Mathieson, S.A., and Wallace, J., 1979, Quaternary tectonics of coastal Santa Cruz and San Mateo Counties, California, as indicated by deformed marine terraces and alluvial deposits, *in* Weber, G.E., Lajoie, K.R., and Griggs, G.B., eds., Coastal tectonics and coastal geologic hazards in Santa Cruz and San Mateo Counties, California: Geological Society of America Guidebook, Cordilleran Section, p. 61-80.

Lemiszki, P.J., and Brown, L.D., 1988, Variable crustal structure of strike-slip fault zones as observed on deep seismic reflection profiles: Geological Society of America, v. 100, p. 665-676.

Leslie, R.B., 1981, Continuity and tectonic implications of the San Simeon-Hosgri Fault Zone, central California: U.S. Geological Survey Open-File Report 81-430.

Lettis, W.R., DiSilvestro, L., Hanson, K.L., and Shiller, G.I., 1990, The San Simeon/Hosgri pull-apart basin; Implications for late Quaternary activity on the Hosgri Fault Zone, *in* Lettis, W.R., Hanson, K.L., Kelson, K.I., and Wesling, J.R., eds., Neotectonics of the south-central coastal California: Friends of the Pleistocene, Pacific Cell, 1990 Fall Field Trip Guidebook, p. 91-138.

Lettis, W.R., Hall, N.T., and Hamilton, D., 1989, Quaternary tectonics of south-central coastal California (abs.): 28th International Geological Conference, Abstracts, v. 2, p. 2-285 to 2-286.

Lettis, W.R., and Hanson, K.L., 1992, Crustal strain partitioning; implications for seismic hazard assessment in western California: Geology, v. 19, p. 559-562.

Lettis, W.R., Kelson, K.I., Wesling, J.R., Angell, M., Hanson, K.L., and Hall, N.T., 1994, Quaternary deformation of the San Luis Range, San Luis Obispo County, California, *in* Alterman, I.B., McMullen, R.B., Cluff, L.S., and Slemmons, D.B., eds., Seismotectonics of the central California Coast Ranges: Geological Society of America Special Paper 292, p. 111-132.

Lewis, K.B., 1980, Quaternary sedimentation on the Hikurangi oblique-subduction and transform margin, New Zealand, *in* Ballance, P.F., and Reading, H.G., eds., Sedimentation in Oblique-slip Mobile Zones: International Association of Sedimentologists Special Publication No. 4, p. 171- 189.

Lowell, J.D., 1972, Spitsbergen Tertiary orogenic belt and the Spitsbergen fracture zone: Geological Society of America Bulletin, v. 83, p. 3091-3102.

Lowell, J.D., 1985, Structural styles in petroleum exploration: Oil and Gas Consultants International Inc., Tulsa, Oklahoma, 477 p.

Lynn, H.B., and Deregowski, S., 1981, Dip limitations on migrated section as function of line length recording time: Geophysics, v. 46, p. 1392-1397.

Mann, P., Draper, G., and Burke, K., 1985, Neotectonics of a strike-slip restraining bend system, Jamaica, *in* Biddle, K.R., and Christie-Blick, N., eds., Strike-slip Deformation, Basin Formation, and Sedimentation: Society of Economic Paleontologists and Mineralogists Special Publication No. 37, p. 211-226.

McCulloch, D.S., 1987, Regional geology and hydrocarbon potential of offshore central California, *in* Scholl, D.W., Grantz, A., and Vedder, J.G., eds., Geology and resource potential of the continental margin of western North America and adjacent ocean basins—Beaufort Sea to Baja Cali fornia: Circum-Pacific Council for Energy and Mineral Resources, Earth Science Series, Houston, Texas, v. 6, p. 353-401.

McCulloch, D.S., and Chapman, R.H., 1977, Maps showing residual magnetic intensity along the California coast, Lat. 37°30'N to 34°30'N: U.S. Geological Survey Open-File Report 77-79, 14 sheets.

McIntosh, K.D., Reed, D.L., and Silver, E.A., 1991, Deep

structure and structural inversion along the central the California continental margin from EDGE Seismic Profile RU-3: Journal of Geophysical Research, v. 96, no. B4, p. 6459-6473.

McLaren, M.K., and Savage, W.U., 1987, Relocation of earthquakes offshore from Point Sal, California (abs.): EOS Transactions, American Geophysical Union, v. 68, no. 44, p. 1366.

McLaren, M.K., and Savage, W.U., 2001, Seismicity of south-central coastal California—October 1987 through January 1997: Bulletin of the Seismological Society of America, v. 91, p. 1629-1658.

Meltzer, A.S., and Levander, A.R., 1991, Deep crustal reflection profiling offshore southern central California: Journal of Geophysical Research, v. 96, no. B4, p. 6475-6491.

Miller, K.C., Howie, J.M., Ruppert, S.D., 1992, Shortening within underplated oceanic crust beneath the central Cali fornia margin: Journal of Geophysical Research, v. 97, no. B13, p. 19961- 19980.

Mount, V.S., and Suppe, J., 1987, State of stress near the San Andreas Fault—implications for wrench tectonics: Geology, v. 15, p. 1143-1146.

Namson, J.S., and Davis, T.L., 1988, Seismically active fold and thrust belt in the San Joaquin Valley, central California: Geological Society of American Bulletin, v. 100, p. 257-273.

Namson, J.S., and Davis, T.L., 1990, Late Cenozoic fold and thrust belt of the southern Coast Ranges and Santa Maria Basin, California: American Association of Petroleum Geologists Bulletin, v. 74, no. 4, p. 467-492.

Niemi, F., Hall, N.T., and Shiller, G.I., 1987, Seafloor scarps along the central reach of the Hosgri Fault southern coast ranges, California (abs.): Geological Society of America, v. 19, no. 7, p. 789.

Pacific Gas and Electric Company, 1974, Geology of the southern Coast Ranges and the adjoining offshore continental margin of California, with special reference to the geology in the vicinity of the San Luis Range and Estero Bay, *in* Appendix 2.5D, Final Safety Analysis Report, Diablo Canyon Nuclear Power Plant: U.S. Atomic Energy Commission Docket Nos. 50-275 and 50-323.

Pacific Gas and Electric Company, 1975, Appendix 2.5E, Final Safety Analysis Report for Diablo Canyon Nuclear Power Plant: U.S. Atomic Energy Commission Docket Nos. 50-275 and 50-323.

Pacific Gas and Electric Company, 1988, Final Report of the Diablo Canyon Long Term Seismic Program: U.S. Nuclear Regulatory Commission Docket Nos. 50-275 and 50-323.

Pollitz, F.F., 1986, Pliocene change in Pacific-plate motion: Nature, v. 320, p. 738- 741.

Reading, H.G., 1980, Characteristics and recognition of strike-slip fault systems: International Association of Sedimentologists Special Publication, v. 4, p. 7-26.

Rietman, J., and Beyer, L., 1982, Bouguer gravity map of California, Santa Maria sheet: California Division of Mines and Geology, 2 sheets, scale 1:250,000.

Sedlock, R.L., and Hamilton, D.H., 1991, Late Cenozoic tectonic evolution of southwestern California: Journal of Geophysical Research, v. 96, no. B2, p. 2325-2351.

Seiders, V.M., 1979, San Gregorio-Hosgri Fault Zone south of Monterey Bay, California—A reduced estimate of maximum displacement: U.S. Geological Survey Open-File Report 79-385, 10 p.

Sengor, A.M.C., Gorur, N., and Saroglu, F., 1985, Strike-slip faulting and related basin formation in zones of tectonic escape—Turkey as a case study, *in* Biddle, K.R., and Christie-Blick, N., eds., Strike-slip Deformation, Basin Formation, and Sedimentation: Society of Economic Paleontologists and Mineralogists Special Publication No. 37 , p. 227-264.

Shen, Z., and Jackson, D.D., 1993, Global positioning system reoccupation of early triangulation sites; tectonic deformation of the southern coast ranges: Journal of Geophysical Research, v. 98, no. 86, p. 9931-9946.

Shih, R.C, and Levander, A.R., 1989, Pre-stack layer-stripping reverse-time migration: EOS Transactions of the American Geophysical Union, v. 70, no. 43, p. 1222.

Sibson, R.H., 1985, Stopping of earthquake ruptures at dilational fault jogs: Nature, v. 316, p. 248-251.

Sibson, R.H., 1986, Brecciation processes in fault zones; inferences from earthquake rupturing: Pure and Applied Geophysics, v.124, nos. 1/2, p. 159-175.

Silver, E.A., 1974, Structural interpretation from free-air gravity on the California continental margin, 35° to 40° N (abs.): Geological Society of America Abstracts with Program, v. 6, no. 3, p. 253.

Slemmons, D.B, 1977, Faults and earthquake magnitude: U.S. Army Corps of Engineers, Waterways Experimental Station, Miscellaneous Papers S-73-1, Report 6, p. 1-129.

Sorlien, C.C., Kamerling, M.J., and Mayerson, D., 1999, Block rotation and termination of the Hosgri strike-slip fault, California, from three-dimensional map restoration: Geology, v. 27, no. 11, p. 1039-1042.

Steel, R., Gjelberg, J., Helland-Hansen, W., Kleinspehn, K., Nottvedt, A., and Rye-Larsen, M., 1985, The Tertiary strike-slip basins and orogenic belt of Spitsbergen, *in* Biddle, K.R., and Christie-Blick, N., eds., Strike-slip Deformation, Basin Formation, and Sedimentation: Society of Economic Paleontologists and Mineralogists Special Publication No. 37 , p. 339-360.

Stone, D.S., 1986, Wrench faulting and Rocky Mountain tectonics: The Mountain Geologist, v. 6, no. 2, p. 67-79.

Sylvester, A.G., compiler, 1984, Wrench fault tectonics: American Association of Petroleum Geologists Reprint Series, no. 28, 374 p.

Sylvester, A.G., 1988, Strike-slip faults: Geological Society of America Bulletin, v. 100, no. 11, p. 1666-1703.

Sylvester, A.G., and Smith, R.R., 1976, Tectonic transpression and basement-controlled deformation in San Andreas Fault Zone, Salton trough, California: American Association of Petroleum Geologists Bulletin, v. 60, p. 2081-2101.

Wagner, H.C., 1974, Marine geology between Cape San Mar

tin and Point Sal, south-central California offshore: U.S. Geological Survey Open-file Report, 17 p.

Weber, G.E., 1983, Geologic investigation of the marine terraces of the San Simeon region and Pleistocene activity of the San Simeon Fault Zone, San Luis Obispo County, California: U.S. Geological Survey Technical Report 66.

Weber, G.E., and Cotton, W.R., 1981, Geologic investigation of recurrence intervals and recency of faulting along the San Gregorio Fault Zone, San Mateo County, California: U.S. Geological Survey Open-File Report 81-0257,131 p.

Weber, G.E., and Lajoie, K.R., 1977, Late Pleistocene and Holocene tectonics of the San Gregorio Fault Zone between Moss Beach and Point Ano Nuevo, San Mateo County, California (abs.): Geological Society of America Abstracts with Program, v. 19, no. 4, p. 524.

Weber, G.E., and Lajoie, K.R., 1979a, Evidence for Holocene movement on the Frijoles Fault near Point Ano Nuevo, San Mateo County, California, *in* Weber, G.E., Lajoie, K.R., and Griggs, G.B., eds., Coastal tectonics and coastal geologic hazards in Santa Cruz and San Mateo Counties, California: Geological Society of America Guidebook, Cordilleran Section, p. 92-100.

Weber, G.E., and Lajoie, K.R., 1979b, Late Pleistocene rates of movement along the San Gregorio Fault Zone, determined from offset of marine terrace shoreline angles, *in* Weber, G.E., Lajoie, K. R., and Griggs, G.B., eds., Coastal tectonics and coastal geologic hazards in Santa Cruz and San Mateo Counties, California: Geological Society of America Guidebook, Cordilleran Section, p. 101-110.

Weber, G.E., and Lajoie, K.R., 1980, Map of Quaternary faulting along the San Gregorio Fault Zone, San Mateo and Santa Cruz Counties, California: U.S. Geological Survey Open-File Report 80-907, 3 map sheets.

Wells, D.L., and Coppersmith, K.J., 1994, New empirical relationships among magnitude, rupture length, rupture width, rupture area, and surface displacement: Bulletin of the Seismological Society of America, v. 84, no. 4, p. 974-1002.

Wilcox, R.E., Harding, T.P., and Seely, D.R., 1973, Basic wrench tectonics; American Association of Petroleum Geologists Bulletin, v. 57, p. 74-96.

Withjack, M.O., Meisling, K.E., and Reinke-Walter, J., 1987, Seismic expression of structural styles; a modeling approach (abs.): American Association of Petroleum Geologists Bulletin, v.71, p. 629.

Wolf, S.C., and Wagner, H.C., 1970, Preliminary reconnaissance marine geology of area between Santa Lucia escarpment and Point Buchon, California: unpub. U. S. Geological Survey administrative report, 5 p.

Woodcock, N.H., and Fischer, M., 1986, Strike-slip duplexes: Journal of Structural Geology, v. 8, no. 7, p. 725-735.

Zaliin, P.V., 1987, Identification of strike-slip faults in seismic sections (abs.): American Association of Petroleum Geologists Bulletin, v. 71, p. 629.